FIELD MEASUREMENTS

L. Bottura, K.N. Henrichsen
CERN, Geneva, Switzerland

Abstract
The measurement of the magnetic field is often the final verification of the complex design and fabrication process of a magnetic system. In several cases, when seeking high accuracy, the measurement technique and its realization can result in a considerable effort. This note describes most used measurement techniques, such as Nuclear Magnetic Resonance, fluxmeters and Hall generators, and their typical range of application. In addition some of less commonly used techniques, such as magneto-optical, SQUIDs, or particle beams methods, are listed.

1. INTRODUCTION

Magnetic systems are designed today thanks to powerful computational tools that achieve remarkable accuracy and are indeed vital for proper optimization. However, the most straightforward way to verify that the required field strength, field shape and desired homogeneity have been achieved is still a direct magnetic measurement. In fact, when striving to reach accuracy in the magnetic field of the order of 100 ppm or better, as needed for example in accelerator and especially NMR magnets, the measurement of the magnetic field is the only way to guarantee that the target is reached. This is especially true when dealing with superconducting magnets, where material properties as well as the magnet geometry are not exactly known at the operation temperature. In addition the magnetic field can be strongly affected by the non-linear, diamagnetic behaviour of the superconducting material.

In addition to magnet technology, the measurement of magnetic fields is a key science in various technical areas. High sensitivity field measurements are used to detect ores underground, mines, submarines in the ocean, heart and brain activity, flux distribution inside superconductors, data stored on magnetic support. Directional field measurements are used to direct vehicles on magnetic tracks, help in the navigation by detecting minute changes in the earth magnetic field, monitor interplanetary activity. Wireless detection of a magnetic field is used to encode and control movements, identify proximity conditions and count items on production lines. Albeit impressive, this is only a much reduced sample of the technical applications requiring sensing and measuring the magnetic field.

This note describes principle and typical applications of most common magnetic measurement techniques and devices. Obviously, given the vastness of the domain, it is not thought as an exhaustive review on magnetic measurement methods. These methods are a typical topic of discussion in dedicated international journals [1], conferences [2,3,4] and workshops [5]. Additional information for researchers as well as new users entering this field can be found in [6] and [7]. In this note we focus mainly on the field measurement methods and devices that are best suited for superconducting magnets and materials, with special attention to operation at cryogenic temperatures, merely listing other interesting or promising methods for the sake of completeness.

2. MEASUREMENT TECHNIQUES

Various different methods are available for the measurement of the magnetic field. The best method for an application can be selected balancing the requirements of the field to be mapped to the typical:

- field measurement range,
- reproducibility and accuracy,

- mapped volume and field geometry,
- time bandwidth

of the method. In addition the measurement environment can impose stringent conditions such as temperature or geometric constraints that can largely drive the selection of the most adapted method. In the sections below we will review the most known field measurement techniques. We will briefly outline the basic principles of the measurement method, discuss the typical measurement techniques and classify the method in terms of range, accuracy, mapped volume and bandwidth.

2.1 Magnetic Resonance

2.1.1 Measurement principle

Magnetic resonance phenomena (Nuclear Magnetic Resonance, NMR, and Electron Paramagnetic Resonance, EPR[1]) provide today the most reliable standards for the measurement of a homogeneous magnetic field commonly achieving accuracy of 0.1 ppm and better in controlled conditions. For this reason NMR is considered today the primary standard for calibration. Nuclear magnetic resonance was first observed in molecular beams in 1938 by Rabi and co-workers [8]. A few years later, in 1946, the phenomenon was observed in liquids and solids by two independent teams [9,10,11].

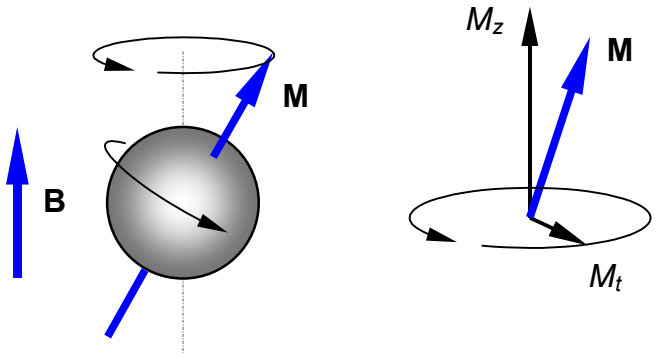

Figure 1. Schematic representation of a particle with magnetic moment in a background magnetic field. The particle precesses with a frequency f. The magnetic moment has a component M_z directed parallel to the external field B and a rotating component M_t in the plane normal to the field.

The principle of the measurement of a magnetic field using magnetic resonance can be intuitively explained starting with the observation that when a particle with a magnetic moment and angular momentum is placed in a background magnetic field with strength B it precesses around the direction of the field, see Fig. 1. The frequency f of the precession, also called Larmor frequency, is proportional to the magnetic field:

$$f = \gamma B \tag{1}$$

where the proportionality constant γ is called the gyromagnetic ratio. This last is a property of the particle that can be traced to standard values such as those reported in Table 1. As an example, for the proton the value of γ is 42.576396(3) MHz/T [12], implying that a proton in a 1 T field precesses at approximately 42.6 MHz.

In general the magnetic moment precession in a sample of many particles is not coherent, and the total magnetization of the sample is parallel to the applied field. It is however possible to use an RF pulse to

[1] Electron Paramagnetic Resonance (EPR) is also referred to in the literature as Electron Spin Resonance (ESR).

rotate the magnetization vectors and achieve coherence. This is the initial step of a typical spectroscopy experiment, when an RF pulse of proper frequency, intensity and direction flips the magnetic moments of the particles. After the end of the pulse the precessing magnetic moments loose coherence in a process called Free Induction Decay (FID). The typical time scale of the FID is determined by spin-lattice and spin-spin relaxation times, and is usually indicated as T_2*. The time constant T_2* can range from a few ms to several seconds, depending on the nature of the sample and specific factors such as the presence of field gradients.

Table 1
Values of the gyromagnetic ratio γ for most common particles and nuclei in magnetic resonance.

particle.	γ (MHz/T)
e^-	28.025 x 10^3
^1H	42.576396(3)
^2H	6.535
^{13}C	10.71
^{14}N	3.08
^{19}F	40.08
^{23}Na	11.27
^{27}Al	11.093
^{31}P	17.25

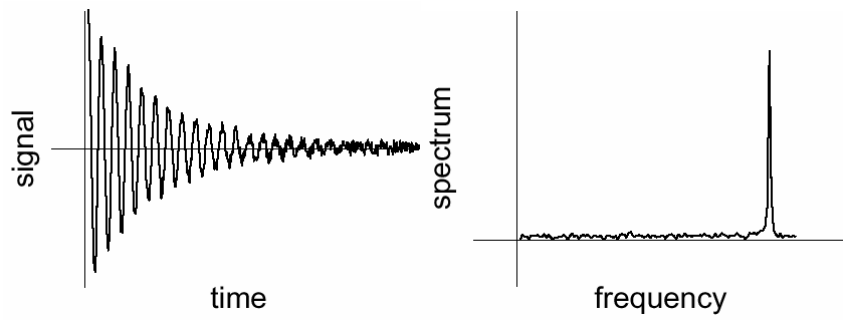

Figure 2. Schematic representation of the signal generated by the decay of the transverse magnetization M_t following an RF pulse (left). The periodic oscillation happening at the Larmor frequency is damped with a time constant T_2* that depends on the nature and state of the sample. A Fourier analysis, schematically shown on the right, gives the oscillation frequency *f* of the nuclear resonance.

Magnetic resonance is very sensitive to the local value of the magnetic field and therefore to field gradients in the sample. A change of the local field in the sample causes a change of the resonant frequency, following Eq. (1). This property is used to achieve encoding of the spatial position through known field gradients in magnetic resonance imaging. However for precise field measurement care must be taken that the field gradient within the resonating sample is kept below tight bounds.

The small field gradients naturally present in a sample made of nuclei bound in molecules are responsible for two other effects that result in a shift of the resonant frequency. Once the nuclei are bound in molecules the field at the nucleus can be affected by shielding (or deshielding) originating from the electron orbitals. This small change in the background field is visible in a shift of the resonating frequency typical of the molecule, called chemical shift. An additional split of the resonant frequency lines is visible when the nuclei are bound closely enough in the molecule. In this case the local field at a nucleus is affected by the alignment of the spin of the neighbouring nuclei. The resulting shift in the resonant frequency is then said to originate from spin-spin coupling. The chemical shift and spin-spin pattern of several molecules is known and can be used as a marker for

spectroscopy. The above effects are small, but become significant and must be taken into account when trying to calibrate the gyromagnetic ratio for a given particle or nucleus to ppb levels.

2.1.2 Field measurement with NMR and EPR

In NMR and EPR devices the measurement of the field is based on the detection and measurement of the precession frequency f of particles contained in a sample placed in the field to be measured. The corresponding field value is then deduced using the proportionality Eq. (1). In general the measurement of a frequency can be performed with very high accuracy, typically fractions of ppm, thus leading to the known accuracy of the method. Different techniques can be used for the measurement of the precession frequency [13]:

Continuous Wave (Q-meter). The sample is inside a coil that is a part of an L-C system tuned on a frequency range f_{min} to f_{max} that determines the range of field B_{min} to B_{max} that can be measured with the probe. The circuit, shown schematically in Fig. 3, is excited by an RF signal, oriented normal to the background field B_0 to be measured. The RF signal initially scans the range of frequency of the probe. When the RF excitation frequency f_{RF} is equal to the precession frequency f_0 for the particle in the external field the L-C circuit absorbs part of the RF signal. This *resonant* condition can be detected by measuring the decrease of the transmission of the RF signal. The corresponding excitation frequency gives then a measurement of the external field through the knowledge of the gyromagnetic ratio. To improve the measurement of the resonant frequency a small, symmetric modulation field ΔB can be added to the background field. The modulation field causes the precession frequency to shift continuously in the range f_0-$\gamma\Delta B$ to f_0+$\gamma\Delta B$. The resonance condition is used in this case to generate a pulse freezing the voltage applied to the field modulation coil. The average voltage during one modulation period is then used as feed-back signal to change the RF frequency. With this expedient the RF excitation f_{RF} is *latched* onto the precession frequency f_0 and thus tracks the external field at all times.

Impedance (Z-meter). Instead of tracking the precession frequency, it is possible to measure a change in the impedance of the sample at the frequency f_0. The sample is in this case a part of a balanced bridge that must include the line between the instrument and the sample itself. At the precession frequency the impedance changes due to the resonance. The change in impedance generates an error signal proportional to the change of phase. Similarly to the continuous wave method, the VCO modifies the oscillation frequency and can thus lock onto the field. As this detection can be faster, this allows faster tracking of a changing field. In addition it can work at higher frequency, in the GHz range, allowing the measurement of higher field strength.

Pulsed Magnetic Resonance. In this case a single RF pulse induces coherence in the magnetic moments. The FID of the sample is measured following the RF pulse and is Fourier analysed to determine the resonance frequency, see Fig. 2. Given the long times available for detection (T_2* can be several seconds) the measurement of the frequency can be very precise in the case of a sample with a single resonant frequency. The interest of this method is that it in addition it can detect resonance at different frequencies as it is the case for particles bound in molecules. In this case the precession frequency is modified by the presence of other particles. For this reason pulsed NMR techniques are commonly used in spectroscopy and imaging techniques.

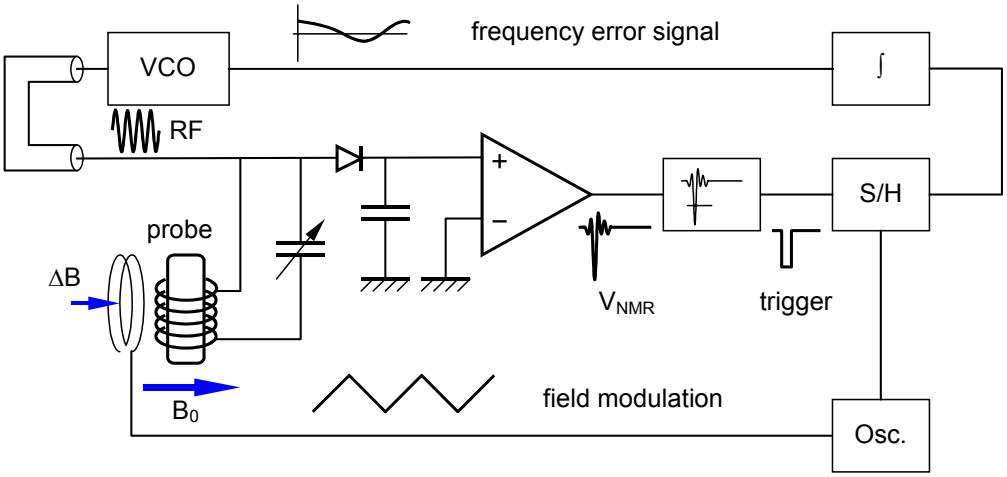

Figure 3. Principle of resonant frequency measurement using the continuous wave (Q-meter). The probe is placed in the background field B_0 and is equipped with an RF excitation coil and a modulation coil that provides the necessary field modulation ΔB for latching the resonance frequency [13].

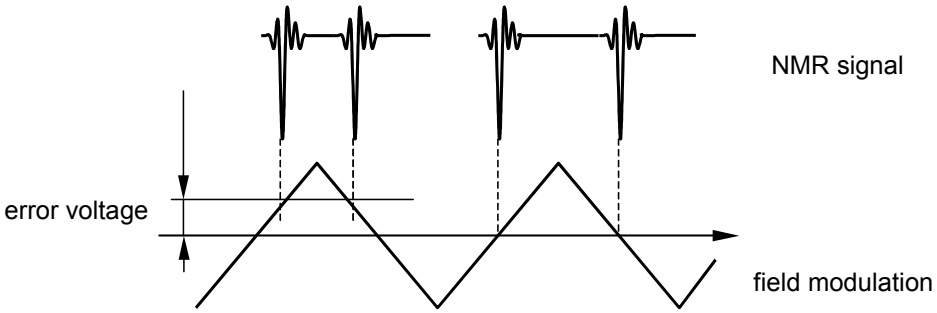

Figure 4. Schematic representation of the latching principle. The resonance peaks detected during field modulation generate an error voltage proportional to the distance of the peaks from the zero-crossing of the field modulation. This error voltage is used to generate a negative feed-back on the RF excitation frequency [13].

Other techniques for special applications. The continuous wave and impedance methods discussed above are the most common techniques for the measurement of uniform magnetic field. In addition, pulsed NMR measurements have been practiced for field mapping in accelerator magnets using a multiple set of samples placed on a circle with the diameter of the bore to be mapped [14]. Probes made from ^{3}He and ^{27}Al have been used even at cryogenic temperatures [15]. The equipment for this type of measurements is at the prototype level and not yet commercially available. Finally, it should be mentioned that a rather exotic method of NMR measurements is to detect the spin resonance in water flowing in laminar conditions in a small tube [16,17,18]. This method has given remarkably good results at low fields for which NMR equipment is not yet commercially available. In addition, it is possible through this technique to perform measurements in environments of strong ionizing radiation such as in particle accelerators. The technique was tested for measurements in the bending magnets installed in LEP, achieving a resolution of 0.1 μT in the range from 0.5 mT up to 112.5 mT [19]. The operation of this type of equipment is rather complicated due to the relatively long time delays in the measurement process.

2.1.3 Range and accuracy

The range of measurement by magnetic resonance is determined by the range of practical frequencies for the electronics of the instrument. Using common RF technology it is possible to detect efficiently a resonance in the 1 to 100 MHz range. Choosing the appropriate material for the probe, the minimum

field that is measured can be as low as fractions of mT (e.g. 0.5 mT using an EPR probe) up to more than 10 T (e.g. 14 T using a deuterium NMR probe). The measurement accuracy depends mostly on the method used to detect the precession frequency and the time taken for the measurement. As a general rule, fast measurements are affected by larger uncertainty on the measured frequency. Continuous wave measurements can reach 0.5 ppm accuracy for 1 s measurement time, and 0.1 ppm for 10 s measurement time. In pulsed NMR the uncertainty on the frequency measured can reach a few ppb, given the long relaxation time available for the data acquisition. A possible source of error is the standard for the gyromagnetic ratio. Although γ is constant in a broad range of temperature, care should be taken to adopt the value that corresponds to the actual state of the particle in the sample. As an example the official value of γ for protons, given by NIST with an uncertainty of 70 ppb, is affected by a 3-ppm shift once the proton is measured in rubber. Once calibration is achieved, however, the knowledge of the value of the gyromagnetic ratio is affected by an error that is much smaller than the resolution of the frequency measurement.

The typical volume of a NMR probe is of the order of 10 to 100 mm^3. The lower limit is set by signal intensity and signal-to-noise requirements and practical manufacturing considerations, while to upper limit comes from the necessity to have a homogeneous field within the probe. One of the most known properties of field measurement through magnetic resonance is that the field needs to be constant in time and uniform through the sample. The effect of a field gradient through the sample is to broaden and lower the resonance peak in the frequency response. This makes on one side latching to the resonant frequency more difficult, while on the other side precision in the determination of the frequency is inevitably lost. The maximum field gradient that can be dealt with depends on the size and material used in the probe and on its range. The limit on the field gradient for a typical probe size with linear dimensions of a few mm is between 10 and 100 ppm/mm. Magnetic fields with higher gradients can still be measured adding small compensation coils. The compensation coils are designed to generate a gradient opposite to the one present in the field to be measured. They are placed around the probe, with the probe centered in the point of zero field. Adjusting the current flowing through the gradient coil it is possible to *shim* the field to be measured thus achieving the desired improvement of the resonance signal. The frequency scan and latching, such as used in the Q-meter technique described above, takes place slowly, typically a few Hz. The corresponding tracking speed is limited in the range of 1 % relative variation rate of field per second. Open loop techniques can be used for faster measurements [13].

2.2 Fluxmeter

2.2.1 Principle

The fluxmeter principle is based on the magnetic induction law in its integral form. If we take the ideal coil of Fig. 5 consisting of a filamentary winding with contour Γ the magnetic flux φ linked with the coil is given by:

$$\varphi = \int_S \mathbf{B} d\mathbf{S} \tag{2}$$

where **B** is the magnetic field, S is an arbitrary surface bound by the contour Γ and d**S** is the normal to the surface. A variation in time of the flux linked by the coil induces a loop voltage proportional to the rate of change, or:

$$V = -\frac{d\varphi}{dt} \tag{3}.$$

A fluxmeter detects this voltage and uses it to measures the flux variation. The magnetic field in the area enclosed by the coil can then be deduced from the flux measurement.

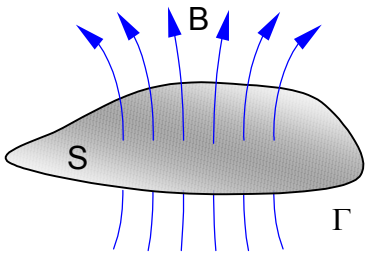

Figure5. Flux linkage with an ideal, filamentary induction coil. The coil contour Γ defines a surface **S**. The flux is defined as the integral of the component of the magnetic field **B** normal to the surface **S**.

The fluxmeter is probably the oldest of the field measurement techniques, and was employed by Weber in the middle of the 19th century to study the direction of the Earth magnetic field [20]. It is a relatively simple method, highly linear, and only requires an induction coil and a voltage measurement. In addition the fluxmeter method provides a very accurate measurement of the field direction, which in some cases (e.g. accelerator magnets) is of greatest importance. As shown in Eqs. (2) and (3) a voltage can be induced on the coil either by a variation of the magnetic field d**B**/dt, or by a change in the orientation of the coil d**S**/dt. In the case of a magnetic field variation in time the coil is usually kept static, and the fluxmeter provides a measurement of the flux change between two given instants. The second technique, i.e. a movement of the coil, is usually employed in static magnetic fields. In this case the field measurement depends, among others, on the precision of the movement. For this reason the most commonly used movements used are simple translations, 180 degrees flip or continuous rotation around a single axis. Fixed and moving coils have been routinely used also for cryogenic measurements.

2.2.2 Measurement of the Magnetic Flux

The measurement of the change of the magnetic flux in a fluxmeter requires forcibly an integration of Eq. (3):

$$\varphi_{end} - \varphi_{start} = -\int_{t_{start}}^{t_{end}} V\,dt \qquad (4).$$

where t_{start} and t_{end} are the time at the start and at the end of the measurement, φ_{start} and φ_{end} are the corresponding values of the magnetic flux. In practice the integration of the coil voltage can be performed using several different techniques:

Analog Integrator. The electronic, analog integrator makes use of the integrating property of an RC circuit. It was the first integrator achieving high speed and good accuracy, and remains today one inexpensive but effective way to measure flux changes. The principle of the electronic integrator, also called Miller integrator, is shown in Fig. 6. For a circuit with ideal characteristics, the signal V_{out} at the output of the DC amplifier is proportional to the integral of the input signal V_{in}. The proportionality constant is $1/RC$:

$$V_{out} = -\frac{1}{RC}\int_{-\infty}^{t} V_{in}\,dt \qquad (5).$$

Connecting an induction coil to the input, and a voltmeter at the output of the circuit it is thus possible to obtain the flux change.

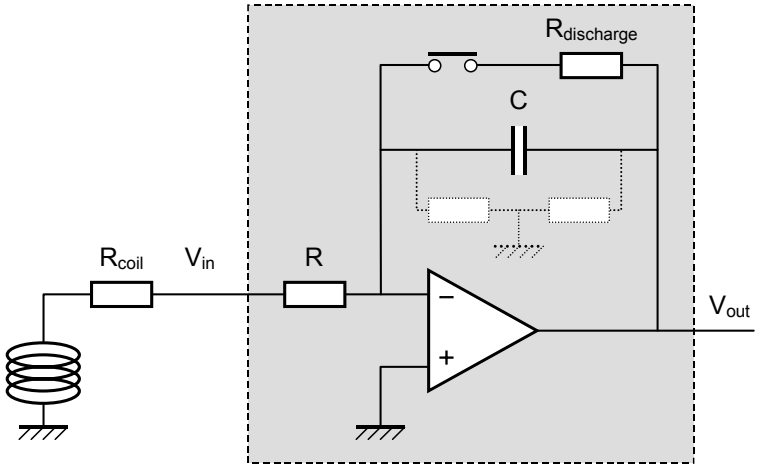

Figure 6. Principle of an electronic analog integrator for the flux measurement. The output signal V_{out} is proportional to the integral of the input signal V_{in}.. Schematically shown the switch and discharge resistor needed to reset the integrator and the parasite resistance responsible for the current leakage between the capacitor plates and to ground.

The most critical element in the analog integrator is the capacitor and in particular the change of its properties with temperature as well as the leakage current. Thermal effects can be controlled through temperature stabilization of the electronics, where the typical level required is better than 0.1 °C. Careful protection and shielding of the capacitor is essential to reduce the voltages across the surface resistances. Another parasitic but important effect is the finite resistance of the coil R_{coil} that acts as an additional load for the integrator, thus changing the proportionality constant between input voltage and output integral. Provided that the effects above are minimised, the limit to the precision achievable with the integrator is then set by the dielectric absorption of the capacitor.

Digital Integrator. A very precise measurement of the flux change can be obtained using hybrid, digital integrators based on the Voltage-to-Frequency Conversion (VFC). The principle of this method, originally developed at CERN, is shown in Fig. 7.

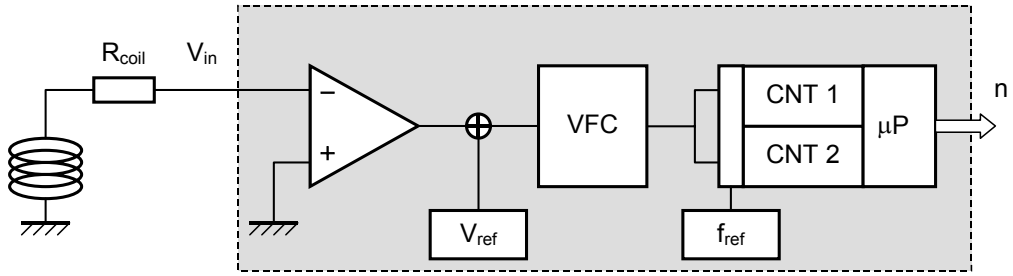

Figure 7. Principle of a digital integrator based on voltage-to-frequency conversion. The digital output n generally available on a computer bus, is proportional to the integral of the input signal V_{in}.

The voltage from the induction coil, after proper conditioning, is sent to a VFC whose output is an AC signal with frequency f proportional to the input voltage V_{in}. The AC signal is then entered in a counter that accumulates the number n of AC pulses during a measurement period starting at t_{start} and ending at t_{end}. The frequency f of the AC signal is equal by definition to the time derivative of the number of

pulses dn/dt, and the output of the counter is, apart for a proportionality constant K_{VFC}, a digital measurement of the integral of the input voltage:

$$n = \int_{t_{start}}^{t_{end}} f dt = K_{VFC} \int_{t_{start}}^{t_{end}} V_{in} dt \qquad (6).$$

The digital integrator achieves high precision thanks to the conversion to frequency domain. The limiting elements in this concept are the stability and linearity of the VFC, and the resolution of counting operation that depends on the maximum operation frequency of the VFC. Hybrid technology VFC's have linearity and stability of better than a few ppm over the whole range of input voltage. The typical maximum frequency of operation is 1 MHz. In order to make the circuit practical some additional features are added to the basic scheme described above. Commercial VFC circuits work only with single polarity voltage, e.g. 0 to 10 V, while the signal from an induction coil can have both polarities. The best way to restore the dual polarity capability is by shifting the input voltage by a precise and stable reference whose effect is to place the input zero exactly in the middle of the VFC range. This offset is then eliminated after counting, subtracting the counts from a reference AC source oscillating at exactly half of the maximum frequency of the VFC. Another technical detail that allows to avoid dead times during the transfer of the result from the buffer of the counter to the downstream circuitry is to use two parallel counters working in alternance. This technique is very effective and results in the cancellation of cumulative errors.

Numerical Integration. Another possibility to integrate the voltage signal from an induction coil is to measure at sufficiently high rate the coil voltage and resort afterwards to numerical techniques. This is possible nowadays thanks to precision Digital Volt-Meters (DVM) or Analog-to-Digital Converters (ADC) commercially available. The principle of a DVM or ADC is to sample the input voltage at a given rate, defined by an electronic trigger. The voltage sample V_i, together with the information on the sampling time t_i and interval Δt_i, can be used to perform numerical integration and thus obtain the flux change at any time during sampling.

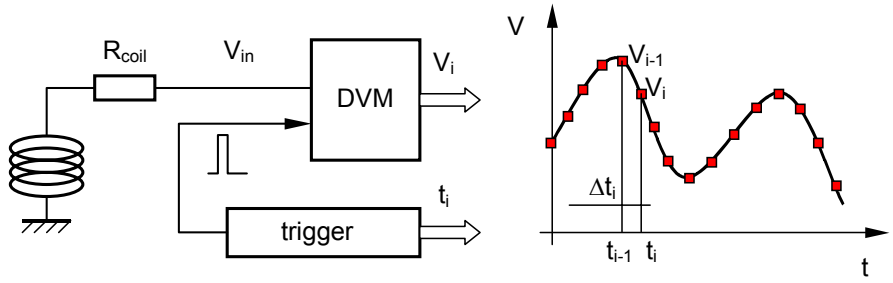

Figure 8. Principle of integration based on digital voltage measurement, showing schematically an approximation for the voltage readings. The DVM delivers instantaneous voltage measurements V_i at precisely defined times t_i. This information is collected by a computer that performs the numerical integration.

The technique is extremely powerful as it can make use of advanced numerical techniques for integration and interpolation. It should be remarked, however, that it generally requires higher sampling rate than analog or digital integration to resolve the fine structure of the voltage waveform in presence of parasitic perturbations or any significant noise. In addition it requires the precise knowledge of the time interval between samples. This can be affected by unknown dead times during data transfer from the DVM or ADC to the following electronics. As for digital integrators it is possible to obviate this last problem by using two voltage acquisitions in parallel and working in alternance.

2.2.3 Induction Coils

The sensor used in a fluxmeter is a stationary or moving pick-up coil. Coils are wound using an insulated conductor of small diameter on non-magnetic and non-conducting support. Suitable supports are composite materials such as fiberglass reinforced epoxy, or amorphous materials such as glasses and ceramics. Mechanical stiffness and low thermal expansion of the support are important requisites to achieve good and stable coil calibration. Similarly the coil winding technique, including the application of proper tension to the wire, is a key point for stable and reproducible results. Finally, good control of the winding geometry is important to calibrate the coil sensitivity to higher order harmonics of the field. High winding uniformity can be achieved using multi-filamentary wire or photo-lithographic techniques [21].

We consider the ideal case of an induction coil of cross section S obtained from N turns tightly wound. The winding can be treated as filamentary if its dimensions are negligible compared to the coil size. If this ideal coil is placed in a uniform magnetic field B oriented normal to the cross section the flux linked with the coil is:

$$\varphi = NSB = \kappa B \tag{7}$$

where we indicate with κ the coil sensitivity that depends on the coil geometry and the number of turns. The number of turns is selected to achieve a sufficient flux linkage to bring the acquisition electronics (integrators or voltmeters) in the useful working range. The flux reading obtained with one of the methods outlined above can be readily converted into field once the coil sensitivity κ is known. In practice the flux linkage depends not only on the field strength and the coil cross-section and number of turns, but also on the shape of the field lines as well as on the coil winding geometry. Different coil geometries can be used depending on the shape of the field to be measured. Often the winding is designed to compensate for field gradients and thus obtain a good measurement of the average field strength in a point or in a cross section. In several cases, however, the coil is specifically built for the measurement of field gradients or higher order harmonics. In all cases the coil sensitivity κ must be determined through an independent calibration procedure.

Coils can be broadly classified based on their form and extension in space as follows [21]:

- point coils, dedicated to the measurement of the magnetic field at a small point in space, ideally infinitesimal;
- line and area coils, used for measurement of integrated field along a line or on a flat region of space;
- harmonic coils, obtained in general as assembly of line or area coils, and designed to be sensitive only to particular spatial harmonics of the field.

Point coil. The simplest point coil is a cylindrical coil wound around a small core. Because of symmetry a cylindrical coil is insensitive to field gradients, and in general to all even field harmonics. Choosing appropriately the ratio of coil thickness to height, as shown in Fig. 9, it is also possible to wind cylindrical coils insensitive to the third spatial harmonic [22]. If the field to be sampled is nearly homogeneous the point coil measures the average magnetic field in the coil volume and can be considered as a close approximation to the ideal case of Eq. (8). A special type of point coil is the fluxball [23]. The fluxball is a coil with spherical shape, wound with a uniform density of turns per unit length along its axis and an increasing density of turns in radial direction, see Fig. 10. This configuration is sensitive to the average field in the sphere and insensitive to all higher order spatial harmonics and can thus be considered as the closest approximation to an ideal point coil. The winding configuration of the ideal fluxball can be approximated for practical purposes using sets of concentric solenoids with appropriate dimensions and turns.

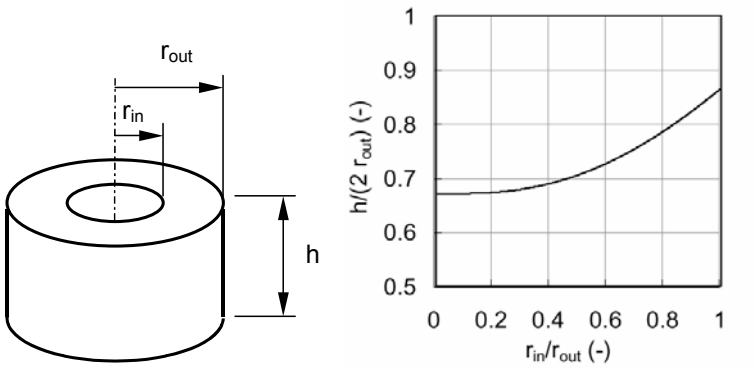

Figure 9. Schematic representation of a cylindrical point coil. The plot shows the ratio of inner to outer radius that cancels the third spatial harmonic of the field, plotted as a function of the ratio of coil height to coil external diameter (from [22]).

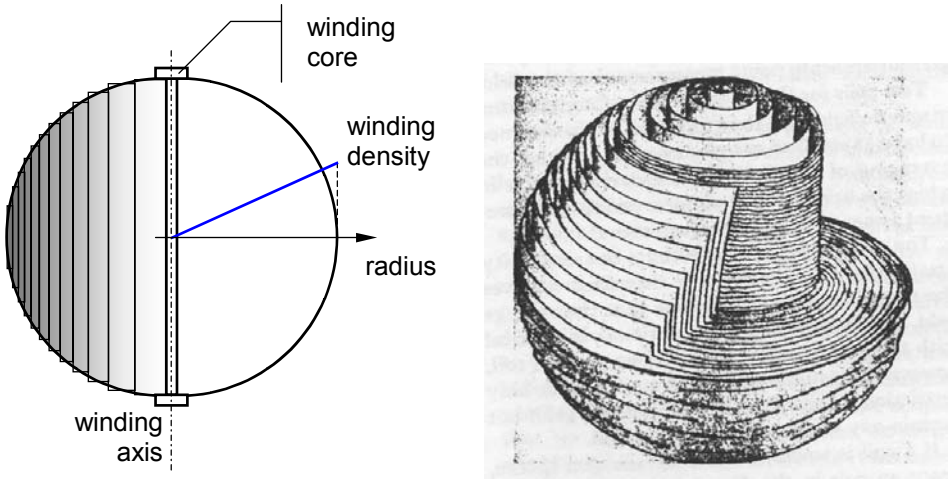

Figure 10. Cross section of an ideal fluxball. The winding density is uniform along the coil axis (vertical) and increases proportionally to the radius across the winding (horizontal). This ideal configuration can be reproduced by proper arrangement of concentric solenoids, as suggested in the picture. Also shown a sketch of its original construction, reproduced from [23].

Line and area coils. Line coils are designed to provide the integrated value of the field along a straight or curved line. Their width is much smaller than the coil length. As for point coils if the winding has a symmetric, rectangular cross section then the flux linked with the coil does not depend on the even harmonics of the field. In addition, by properly selecting the ratio of winding thickness and height the coil can be made insensitive to the third spatial harmonic [24,21]. Any coil that has comparable winding width and length or height can be classified as area coil. Area coils have the same properties of line coils, but they sample a large area of space. Line and area coils of long length and slender construction are routinely used for the measurement of the field in accelerator magnets. The reason is that in spite of their considerable length (e.g. 15 m for the LHC dipoles) the effect of an accelerator magnet on the particle beam, whose betatron oscillation happens on a much longer scale, can be assimilated to a localised optical element of equivalent strength and negligible dimension. Under this condition it is enough to know the integrated field strength and homogeneity of the magnet under examination. Long rectangular coils, translated horizontally during the measurement, were usually employed and are still used in magnets with a wide horizontal aperture and limited gap height. Similar coil geometries are used for rotating coils measurements in the narrow, circular bore of superconducting accelerator magnets. A few typical examples are shown in Fig. 11.

Figure 11. Examples of typical induction coils used for accelerator measurements, by courtesy of J. Billan (CERN). The coils have length ranging from 25 cm to more than 2 m much larger than its extension in the cross section (10 mm to 50 mm), and windings of negligible dimensions with respect to the overall size of the coil (typically 0.5 x 0.5 mm).

Harmonic coil. Shaping the coil winding, or interconnecting coils suitably placed in space, it is possible to achieve sensitivity only to a selected number of spatial harmonics of the field. We call such a winding or set of windings a harmonic coil. Harmonic coils are a particularly useful expedient when investigating the field homogeneity. Indeed the sensitivity to field errors can be largely increased if the main field component is cancelled using a suitable array of coils. A simple example of a coil only sensitive to even harmonics is a *gradient* coil, consisting of a set of two identical windings mechanically mounted either side by side or on top of each other and wound in opposite direction. The total signal from the gradient coil is insensitive to the average field, as the signal produced by the two windings is identical in amplitude and opposite in sign. A field gradient, instead, produces signals of identical amplitude and sign on both windings thus resulting in a net output. Another example of harmonic coil that has been used in the measurement of the two-dimensional field of accelerator magnets is the Morgan coil [25]. The coil winding in a Morgan coil is subdivided in $2M$ blocks that are placed with uniform angular spacing on a cylinder. The contiguous blocks have opposite winding direction and form M ideal loops connected in series. This configuration is only sensitive to harmonics of order $(2k+1)M$, with k integer. An example of the cross section of a Morgan coil sensitive to the octupole harmonic B_4 (fourth harmonic $M=4$) is shown schematically in Fig. 13.

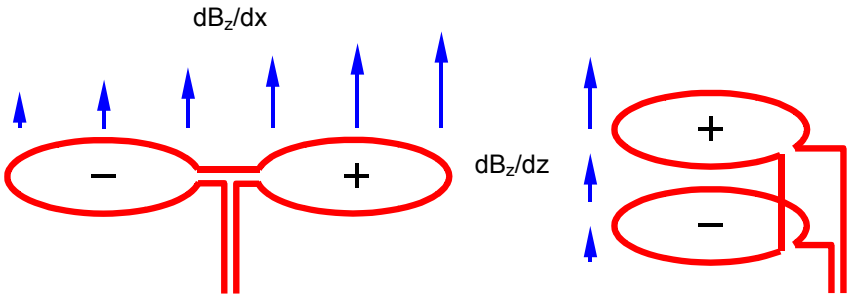

Figure 12. Schematic representation of different coils sensitive to a field gradient in the vertical component of the magnetic field B_z. Gradient coils are used to measure the second spatial harmonic of the field.

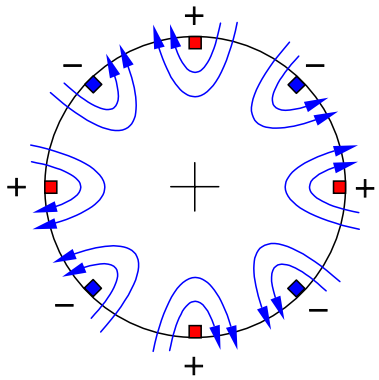

Figure 13. Cross-section of a Morgan coil sensitive to the fourth harmonic of the field (M=4, octupole term B_4). The winding direction enters or exits the plane of the page alternatively, according to the signs indicated. Also shown schematically the field lines for an octupolar field.

2.2.4 Coil calibration

One of the main sources of error in the fluxmeter is the uncertainty on the sensitivity of the coil to the field measured. Because of tolerances and imperfections during coil manufacturing the real winding shape has inevitable deviations from the ideal one. The solution is to calibrate the coil in reference magnets using a field reference such as an NMR probe. In addition to the equivalent surface of the coil it is often necessary to measure the orientation of its median plane with respect to mechanical references on the coil support. This is a mandatory calibration step if the coil has to be used for the measurement of field direction. Gradient coils are calibrated in magnets with known gradients or alternatively using controlled displacements in an unknown gradient magnet. Erratic signals from wire loops must be avoided during the calibration process as well as during measurements. In case that the field to be mapped has strong variations along the length of the coil, it may be necessary in addition to examine the change of the effective width. Temperature variations and long term geometric stability can affect the quality of the calibration that may thus require periodic checking. For cryogenic applications, and especially at liquid helium temperature (4.2 K), it is necessary to take into account the large thermal contraction from room temperature to the measurement conditions (several 1000 ppm in terms of coil surface). This is usually done either using empirical contraction coefficients or calibrating at liquid nitrogen (77 K) and neglecting the residual thermal contraction below 77 K. Precise calibration at cryogenic temperature is for obvious reasons more difficult to achieve and leads to an overall decrease in the expected accuracy.

2.2.5 Field measurement with fluxmeters

As we anticipated, the field measurement using a fluxmeter is generally performed either keeping the induction coil fixed, in case of changing field, or moving the coil in a static field. In the case of fixed coil measurements, the integrator is reset at the start of the measurement (e.g. discharging the capacitor in the analog integrator). In the simplest case the integration starts and continues till the end of the measurement, when the flux change is finally readout. The flux change is then converted to the desired value of field change using the known coil calibration, e.g. the surface for a uniform field as in Eq. (8). Note that according to Eq. (4) a fixed coil measurement can only give the flux *change* between the start and the end of the measurement and is therefore an intrinsically relative measurement. Indeed, an absolute measurement is possible only in the case that the magnetic field at the start is known to be zero. In practice the integrator can be readout or electronically triggered to deliver the flux change at any desired time during the measurement period, thus providing the waveform of the field change. For fixed coil measurements it is of primary importance to reduce the voltage offset at the input of the integrator generated by parasitic currents in the electronics or thermal voltages. An input voltage offset translates in an apparent field drift that often cannot be distinguished from the physical field change. This effect becomes important for long integration times, normally a few seconds to minutes for state-of-the art technology. Offset trimming must be performed electronically in well-controlled steady-state conditions (i.e. when the induced voltage on the coil is zero) and is often supplemented by digital reduction of residual drift. The latter is possible if the measurement spans phases when the field is constant, and the input voltage of the integrator is thus the residual offset, in addition to the period of changing field, when the input voltage contains both contributions from induced voltage and offset.

When the field is constant the necessary induction signal is generated moving the induction coils. The integrator is reset before the movement and is readout at the end of the movement. Because the magnetic field is solenoidal, the final reading depends only on the initial and final positions of the coil and does not depend on the path taken for the movement. Starting with the coil outside the magnet (e.g. in a zero-Gauss chamber) and finishing with the coil in the magnet bore, the initial field is known to be zero so that the total flux change can be used to deduce the absolute value of the field. This *moving coil* technique has been successfully used to measure field strength in accelerator dipole magnets taking care that the final position of the coil is normal to the field. An alternative technique consists in *flipping* the coil, rotating it by 180 degrees during the measurement. In this case the flux change during the measurement is equal to twice the flux linked with the coil in the initial position. Taking again the case of a homogeneous, dipole field as an example, and having placed the coil initially normal to the field, it is possible to use the flux change to deduce the absolute field strength. As in the case of fixed coil measurements, both moving and flip coil techniques are sensitive to the adjustment of the voltage offset. In these cases however the initial and final states are by nature stationary and it is easier to identify residual drifts. In addition first-order drift correction can be obtained by proper combination of movements including direction reversals, thus exploiting physical symmetries. Finally in both cases the resolution can be greatly increased by using differential measurements, where a pair of coil is connected in opposition, with one coil moving and the other stationary. This expedient can be used to compensate fluctuations in the magnet excitation current and to provide higher sensitivity when examining field quality.

An alternative method based on induction measurement is the *stretched wire* technique [26,27] that can be regarded as an extension of the moving coil. In its simplest variant a thin wire of high strength, non-magnetic material (e.g. W or CuBe) is stretched inside the bore of the magnet. A second wire, laid fixed either inside the bore or outside the magnet, provides the return path for this single-turn coil. The stretched wire is moved in the magnetic field using precision stages and the signal generated by the flux cut during the movement is integrated as in the case of a moving coil. The accuracy in this case is mainly determined by the precision of positioning. Sensitivity and resolution can be increased using

multi-wire arrays. This method is well suited to geometry measurements, to the absolute calibration of quadrupole fields and in particular to measurements in strong magnets with very small aperture.

Rotating coils is finally one of the most successful methods in the measurement of field and field quality for accelerator magnets. Devised since 1954 [28,29] the method has become now widely used for magnets with cylindrical bore. The induction coil is placed on a circular support and is rotated in the field to be mapped. The coil angular position is measured by an angular encoder, rigidly connected to the rotating support. As the coil rotates in the field it cuts the flux lines and a voltage is induced at the terminals. Integrating the induced voltage between predefined angles using one of the techniques described above it is hence possible to obtain the flux change as a function of angular position, as shown schematically in Fig. 14. If the field measured is 2-D in the cross section of the magnet measured, with negligible variation along the magnet length, it can be shown [30] that a Fourier analysis of the angular dependence of the measured flux leads naturally to coefficients directly proportional to the so-called multipole coefficients of the field [31]. In turn the multipole coefficients of the field can be related directly to linear and non-linear accelerator beam properties, thus explaining the wide acceptance of the rotating coil method for mapping accelerator magnets.

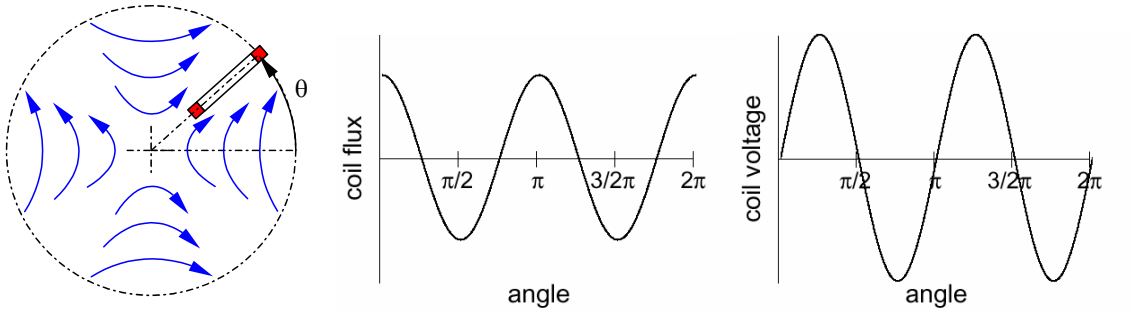

Figure 14. Principle of the rotating coil method showing an induction coil rotating in a quadrupole field and the corresponding flux and induced voltage plotted as a function of angular position θ.

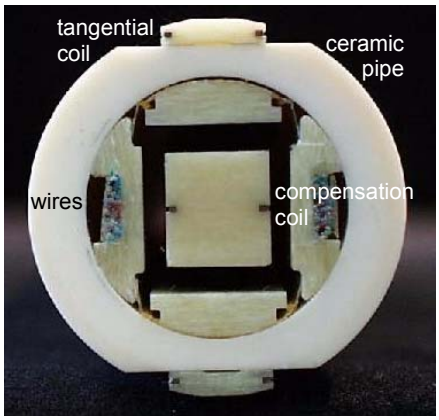

Figure 15. Cross section of the rotating coil used at CERN for the measurement of the 15-m long superconducting LHC dipoles. The upper and lower coils, mounted on a hollow ceramic haft, are used for the measurement of the main field strength and direction. The signal from the central coil is used to compensate analogically the contribution of the dipole component without affecting higher order harmonics.

In order to facilitate the realisation of a practical rotating coil system the angular encoder can be used to trigger the integrator so that integrator delivers the flux change between adjacent angular positions. This method eliminates the time dependence and in particular the influence of variations of the rotation speed, greatly relaxing requirements for uniform rotation. Differential measurements are also greatly beneficial to increase the resolution of high-order multipoles, generally several orders of magnitude smaller than the main field in an accelerator magnet. This is realised using a set of

compensation coils mounted on the rotation support. The signal from the compensation coils is used to suppress the strong contribution from the main field, either analogically or digitally. The residual signal, usually called *compensated* or *bucked* signal, can be analysed in Fourier series to obtain the higher order multipoles. A cross section of a typical rotating coil is reported in Fig. 15, showing the arrangement of main and compensation coils on the stiff ceramic support. The signal from the rotating coils is transmitted either through slip-rings or through flexible cables to the integrator. In the first case the coil can rotate continuously in one direction, while in the second case it must be returned to the start position. Using this return rotation for a *backward* measurement, and averaging its result to the one obtained during the *forward* rotation it is possible to draw advantage from this "*washing-machine"* operation to reduce systematic errors such as those due to mechanical torsion.

2.2.6 Range and accuracy

An induction coil is a linear device, whose sensitivity can be designed to fit the field to be measured. Hence the fluxmeter is a method potentially covering a very broad range of field measurement. Its main limitation originates from thermal and environmental noise, electronic drifts and the quality of the mechanics in the case of moving or rotating coils. In practice the application of the induction method is limited to minimum field levels above 0.1 μT, with no fundamental limitation at the upper end.

The first error source in a fluxmeter is the coil sensitivity. Coil sensitivity to a uniform field, i.e. the effective surface, can be calibrated to typical accuracy ranging from 10 to 100 ppm, depending on the size and shape of the coil. Gradient coils can be calibrated to better than 1000 ppm. The accuracy of integration depends strongly on the integration technique used. Analog integrators reach accuracy of 100 ppm and resolution of a few ppm. The resolution is generally limited by the noise and offset of the input amplifier. Digital integrators can reach linearity of better than 10 ppm and overall accuracy of 100 ppm. The resolution of digital integrators is affected by noise and offset of the input amplifier and in addition depends on the discretization noise of the counters. This last usually imposes the most severe limit, resulting in a resolution proportional to the clock frequency and to the inverse of the integration time. As an example, a digital integrator with a 1 MHz clock and integrating for 1 s has a resolution of 0.25 ppm. If the integration time is reduced to 1 ms the resolution decreases to 250 ppm. For DVM's and ADC's the accuracy of the reading can be very high, of the order of 1 ppm and better, and the digital stage is usually sized not to limit the resolution of the reading. In this case the largest error source comes from the jitter in the integration time intervals, from uncorrected dead time during reading and from the numerical approximation of the voltage integral. Overall accuracy of numerical integration methods is then comparable to the performance of digital integrators, in the 100 ppm range.

The volume sampled by induction coils can also be vastly different. Coils can be practically wound around a 1 mm^3 core to sample point regions. At the other extreme rotating coils with diameter in excess of 1 m have been used to sample a few m^3 of space. The time response of the fluxmeter depends on the bandwidth of the electronics reading and integrating the coil signal. In the case of analog integrators and numerical integration the voltage readout can be fast, up to 50 kHz For digital integrators the balance among integration time and resolution usually limits the acquisition frequency to the range of 100 Hz.

2.3 Hall generator

2.3.1 Principle

Hall generators measure the magnetic field through its effect on the free path of charge carriers in a conducting or semi-conducting material. In a Hall generator an electric current flows in a small section of a suitable material placed in the region where the magnetic field **B** must be mapped. For simplicity

we assume here that the material is a thin slab and we consider only the magnetic field component $B\cos(\theta)$ normal to the wide face of the slab, as shown in Fig. 16. The charge carriers moving in the material are subjected to a force **F** transverse to the direction of the electric current, with a magnitude:

$$F = qvB\cos(\theta) \tag{8}$$

where q is the charge of each carrier and v the average drift velocity of the carrier. This force tends to curve the direction of flow of the charge carrier and causes the polarization of the material in the direction of **F**. The resulting electric field, whose effect at equilibrium balances the transverse force from the applied magnetic field, is the Hall voltage. The magnitude of the Hall voltage V_H is proportional to the magnetic field component normal to the surface of the generator and to the electric current I exciting the Hall generator:

$$V_H = GR_H IB\cos(\theta) \tag{9}$$

where θ is the angle between the direction of the field and the normal to the generator, the factor R_H is the Hall coefficient characterizing the material used in the generator, and G is a geometric factor depending on the size and shape of the generator itself. It is interesting to remark that, in accordance with Eq. (9), the Hall generator provides a steady-state signal proportional to the magnetic field.

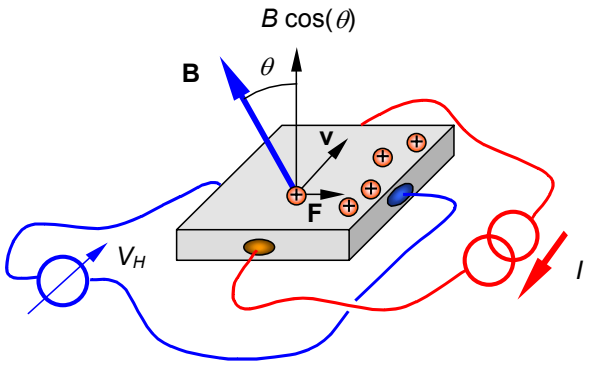

Figure 16. Schematic representation of the force acting on majority charge carriers (assumed to be holes in the example considered) in an ideal Hall generator and appearance of the Hall voltage.

The Hall effect [32] was firstly observed in metals, such as iron, gold and silver. The Hall coefficient of these materials, the ratio between transverse voltage and applied magnetic field, is relatively small. In an ideal Hall generator the Hall coefficient is proportional to the mobility of the charge carriers in the material, and inversely proportional to its conductivity. Because metals exhibit low mobility and high conductivity they are not suitable for efficient Hall generators, and in principle low conductivity materials should be preferred. On the other hand, and especially for temperature stability reasons, it would be preferable to use materials with a small resistance to the flow of the control current. It was only with the use of semiconductors [33] that the right balance could be achieved among mobility and conductivity and Hall generators became practical for field measurement. Nowadays Hall generators are built using either un-doped semiconductors such as Si or compounds of the type $A^{III}B^{V}$, i.e. formed by elements of groups III and V of the periodic table, such as InSb, InAs and GaAs.

2.3.2 Non-linearity and parasitic effects

Practical Hall generators are fabricated using the same technology applied for the production of thin semiconductors, often directly within integrated circuits that provide sturdy packaging and easy connection through soldering pads. Because of their finite, small dimension the flow of current within the material is much more complex than the simple picture discussed above. The terminals connection

act as discontinuities perturbing the current flow (current terminals) or affecting the voltage pick-up. When the size of the connections is large with respect to the dimension of the Hall generator itself, the connections can partially shunt the current and thus deform the ideal electric field pattern.

The finite geometry of the contacts and the shunting of the Hall voltage influence the electric field pattern in different ways a different applied magnetic field. As a result a Hall generator has a non-linear response to the field, usually identified as a field dependence of the geometric factor G. In addition to this geometric non-linearity, a Hall generator has also a material non-linearity that is commonly attributed to the Hall coefficient R_H. By proper choice of geometry and material it is possible to partially compensate the two effects achieving linear response to better than 1 % over a wide range of field. In this respect the Hall generator of the cruciform type [34] shows a better linearity and has a smaller active surface than the classical rectangular generator. Its magnetic center is better defined, so that it is particularly well suited for measurements in strongly inhomogeneous fields.

Another source of non-linearity in the characteristics of Hall generators is the variation of temperature. Both the charge mobility and material conductivity are temperature dependent, so that the Hall coefficient R_H has a temperature dependency that can be of the order of 100 to 1000 ppm/°C. The control current in the Hall generator is associated with a small heat source that must be controlled to achieve high precision.

As discussed above, the voltage reading in a Hall generator depends on the direction of the magnetic field. The maximum Hall voltage is measured when the magnetic field is in a direction normal to the generator, and ideally the Hall voltage is zero when the magnetic field is in the plane of the device. In reality any anisotropy in the generator leads to a non-zero voltage also when the field is in the plane of the sensor. This effect is often referred to as *planar* Hall effect, and depends on the field strength and on the angle φ between the field and the direction of the electric current in the generator [35,36,37] giving rise to an additional voltage at the terminals:

$$V_{planar} = V_{HP} B^2 \cos(2\varphi) \tag{10}$$

where V_{HP} is a coefficient typical of the material used and of the geometry of the generator. The typical planar Hall voltage in a generator built with InSb semiconductor is shown in Fig. 17.

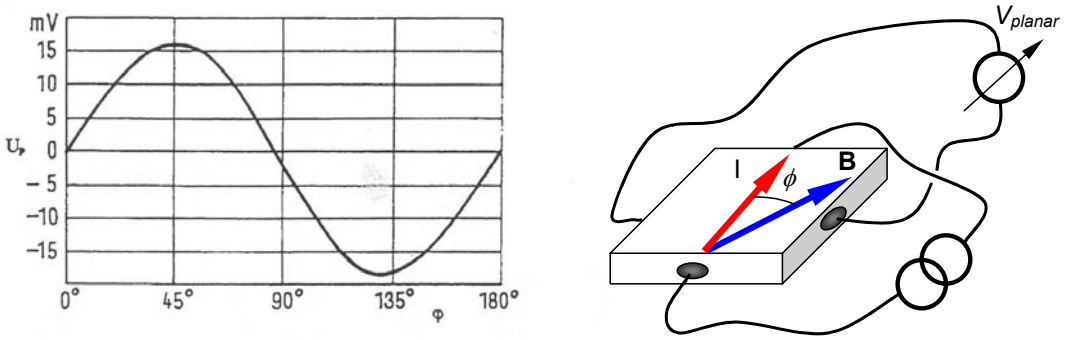

Figure 17. Measurement of planar Hall voltage in an InSb Hall generator in a background field of 1 T, plotted as a function of the angle between the field and the direction of the current in the generator (reproduced from [37]).

Magnetic field gradients can also have an effect on the Hall voltage, mainly because the generator has a finite size. The effect of field variation in the sensitive region of a Hall generator is however small and is generally neglected [36].

Special Hall generators for use at cryogenic temperature are also commercially available. Although they show a very low temperature coefficient, they unfortunately reveal an additional problem at low temperatures. In these conditions the so-called Shubnikov-de Haas effect [38,39] is responsible for a field dependent oscillation of the Hall coefficient causing as a deviation from the linear sensitivity. The deviation may amount to about one per cent at high fields, depending on the type of semiconductor used for the Hall generator. An example of this effect is shown in Fig. 18. The Shubnikov-de Haas effect adds a serious complication to the calibration.

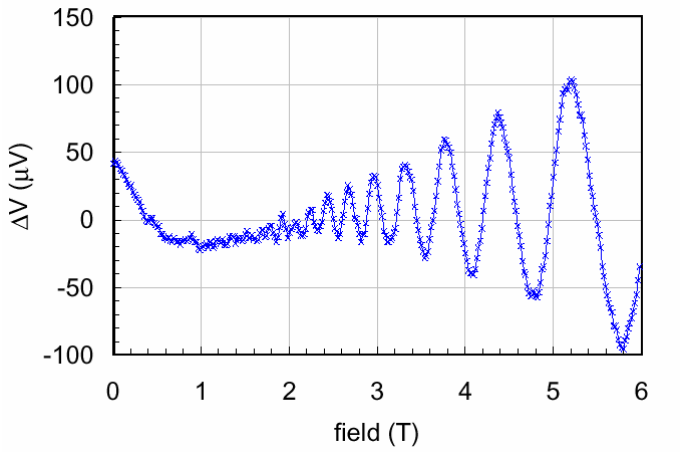

Figure 18. Shubnikov-de Haas effect in a Hall generator at 4.2 K. The plot shows the deviation ΔV of the Hall voltage from a straight line as a function of the applied field. For comparison, the Hall generator produces on average 10 mV/T.

A further parasitic effect is associated with the presence of a voltage offset even at zero applied magnetic field. The offset can be of geometric origin (misalignment of the voltage terminals with respect to the electric equipotential lines), associated with rectifying effects at the metal-semiconductor connection, stress induced or originating from gradients in material properties (e.g. doping density). The offset voltage is temperature dependent, and in addition temperature gradients at the connections can generate thermo-electric voltages. Voltage offsets can be significant, 0.1 to 1 mV are typical values, and hence need to be controlled or compensated to achieve good precision.

2.3.3 Field measurement with Hall generators

A Hall generator is a four-terminal device. The control current is generally supplied by a highly stable AC or DC source, while the Hall voltage is read by a high impedance voltmeter or is fed to the acquisition electronics (amplification or conditioning). It is useful to remember that the Hall generator input is not isolated from the output. In fact the impedance among input and output is generally of the order of the input resistance. In practice the current source must be isolated from the electronics that reads the Hall voltage to prevent stray current flowing through the Hall generator in the electronics. This is often achieved using a differential-input amplifier for signal conditioning.

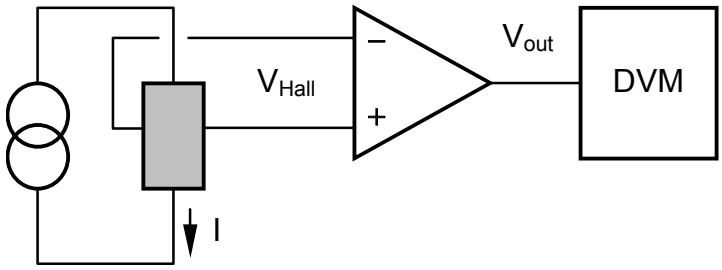

Figure 19. Principle of use of a Hall generator showing the current source and readout electronics.

AC excitation and lock-in techniques are used to increase the noise rejection of the reading of the Hall voltage. In this case the source current is modulated while the voltage is readout synchronously with the excitation. The frequency of the excitation is low, a few Hz to a few hundred Hz, and is chosen to reject typical sources of systematic noise such as 50 Hz and the related harmonics.

The measured Hall voltage must be converted to the value of the field using a calibration function. To achieve precision of the order of 1 % and better this function must be established through an independent measurement in a known field. The non-linearity in the relation between field and Hall voltage is in fact one of the major drawbacks of Hall generators. Precision measurements require in addition the knowledge of the temperature and the relative correction of the calibration. Alternatively, temperature compensation in a thermostat surrounding the Hall generator can be used. In this case the calibration measurement is performed at the same working temperature.

Another major issue to be considered for the calibration and the measurement is the alignment of the Hall generator. The Hall generator is a directional device, sensitive to the field component normal to the generator. An angle between the field and the normal to the surface of the generator results in an apparent reduction of the field strength. This can be empirically corrected by tilting the Hall generator until the maximum reading is obtained. Alternatively, one can establish a mechanical reference that can be reproduced between calibration and measurement. Three-dimensional arrays of Hall generators, also available as single chips sensitive to the three components of the magnetic field, once complemented with a suitable calibration, are the best adapted devices for field strength measurement.

Finally, it is important for precision measurements that parasitic effects, and especially voltage offset, are minimised or compensated. The offset is best removed with the Hall generator placed in a zero-field chamber, providing an ideal volume with no magnetic field. The offset compensation can be electronic or digital. In any case temperature stabilization is necessary to prevent the drift in the offset caused either by changes in temperature or temperature gradients.

2.3.4 Range and accuracy

Thanks to the latest technological development in integrated circuit design and manufacturing, Hall generators have become inexpensive devices that are widely used for large-scale applications and field mapping. The directionality and small active area of the Hall generator make it to an ideal instrument for mapping magnetic fields in a very wide range of strength and shape. Other attractive features are the wide dynamic range and the possibility of static operation under constant excitation current. The range of field that can be practically measured is related to the voltage measurement capability and the sensitivity of the Hall generator. The sensitivity in turn varies depending on the material, the thickness of the generator and the size of the active area. Commercially available generators have typical sensitivities in the range of 10 mV/T to 1 V/T. The typical field measurement range for these generators is above 1 mT. Accurate voltage measurement is possible below the μV level using precision voltmeters, thus giving a field resolution better than 0.1 μT.

The absolute accuracy of the measurement is mostly governed by the non-linearity and its temperature dependence, alignment errors, and the parasitic effects discussed earlier. Commercial equipment has typical accuracy 1000 ppm of reading. Custom-made calibration, temperature control and various compensation techniques can be used to achieve an improvement of a factor 10, giving an absolute accuracy of 100 ppm of reading. An additional issue in Hall generators is long-term stability. A well-designed Hall-probe assembly can be calibrated to a long-term accuracy of 100 ppm. The stability may be considerably improved by powering the Hall generator permanently and by keeping its temperature constant.

The active area of the Hall generator determines the size of the volume mapped. Typical volumes are in the range of 0.01 mm^3 to 0.1 mm^3. Quoted time resolutions for Hall generators are below 1 ns, as typical of semiconductors electronics. In general however the main measurement bandwidth limitation is determined by the precision voltmeter. Commercial devices have maximum bandwidth extending up to 500 Hz.

2.4 Magneto-resistors

Conducting materials exhibit a change in resistivity once exposed to a magnetic field. This effect, discovered by W. Thomson in mid 19th century [40], was exploited to measure the strength of the field already at the beginning of the 20th century. The change in resistance in conductors is due to two contributions, a *physical* contribution related to the intrinsic conductance properties of the material, and a *geometric* contribution due to the bending of the carrier path under the magnetic force and thus of the same origin as the Hall effect. The magneto-resistance associated with intrinsic changes in conductance property is usually small at room temperature, of the order of 0.5 to 2.5 % increase at 1 T in semiconductors such as InSb and InAs that are commonly used to build magneto-resistors. The origin of the geometric contribution is of dual nature with respect to the Hall effect and can be successfully exploited by properly shaping the current path in the material.

To explain how this is done we need to recall that in a Hall generator the bending of the current flow gives rise to a polarization in the direction transverse to the current. At a sufficient distance from the electrodes, and once the transverse electric field has built up, its effect is to balance the force due to the magnetic field. Therefore in a Hall generator in steady-state operation the current path is nearly straight between the two terminals, and the resistance has only a modest variation with field.

If, on the other hand, the Hall generator is built with a very short length then the charge cannot build up at the sides, and the transverse field is negligible while the current path curves increasingly as a function of the applied field. In this situation the Hall voltage is small while the longitudinal resistance increases significantly with field due to the increase of the length traversed by the charge carriers. To reach an appreciable total resistance, and thus improve the sensitivity to the magnetic field, several of these short Hall generators must be piled in series. One of the possible ways to achieve this is to distribute microscopic needles of a high conductivity material such as NiSb in a base material with large Hall effect such as in InSb. The needles are placed with their long axis normal to the current flow and thus short the Hall voltage transverse to the current. In practice the needles delimit ideal Hall plates with a small ratio between width and length, as shown schematically in Fig. 20. The change in the length of the current path under the action of the magnetic field between two adjacent needles is responsible for the increase in resistance.

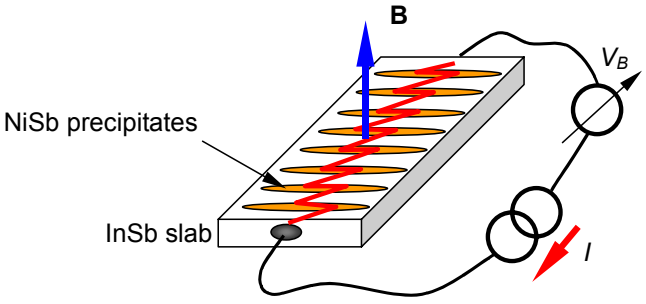

Figure 20. Schematic representation of a magneto-resistor containing needle-shaped low resistance precipitates (e.g. NiSb) in a semiconductor matrix (e.g. InSb). The needles act as shorting bars for the Hall voltage, and redirect the current flow, shown as the *zig-zag* path inside the slab. The total resistance growth with field is proportional to the change in the length of the current path in the semiconductor.

Magneto-resistors of this type have a highly non-linear resistance increase, in first approximation proportional to the square of the field strength, or:

$$\frac{R_B}{R_0} \propto B^2 \tag{11}$$

where R_0 and R_B are the resistances in zero field and in the applied field respectively. For this reason magneto-resistors are relatively insensitive to low fields. In addition they are sensitive only to the field component in the direction normal to the slab, but cannot distinguish field polarity. Finally they have large temperature coefficients, 2500 ppm/C typical, and can be affected by large property variations from device to device. For the above reasons up to recent years magneto-resistors did not find widespread application, in spite of the advantage of being a two-terminal device and the easy manufacturing with integrated circuit technology. The recent discovery of the *giant magneto-resistance* effect [41] as well as technological developments have improved the situation. Highly symmetric magneto-resistors are built today using thin layers of ferromagnetic and non-magnetic materials in Wheatstone bridges for high sensitivity detection of magnetic field gradients. The symmetry is achieved by manufacturing the magneto-resistors using photolithography on the same substrate. The resistive bridge configuration largely removes temperature dependence of the balanced voltage, as well as the effect of uniform magnetic fields. Often a magnetic element is added in the circuit to produce a bias field that displaces the working point of the magneto-resistors to a region of acceptable linearity. In this configuration magneto-resistors can be used as position and proximity sensing devices, as well as devices to measure the electrical current in nearby conductors. In this range of applications magneto-resistors are suitable for the detection of fields in the range of 1 μT to a few mT. In resistive bridge configuration, using suitable feed-back circuitry for compensation, the sensitivity can be as low as 100 pT. Calibration properties and long term stability are similar to Hall generators, although the intrinsic non-linearity of the sensors lowers the absolute precision that can be achieved to the level of fraction of % (1000 ppm). The typical bandwidth of magneto-resistive sensor is extremely large, from DC to several GHz, and the volume mapped can be extremely small, down to 100 μm^2, e.g. for photo-lithographically patterned giant magneto-resistive sensors.

2.5 Fluxgate magnetometer

A fluxgate magnetometer measures the magnetic field through its effect on the magnetization of a thin ferromagnetic core with a very high magnetic permeability and nearly rectangular hysteresis. The measurement principle is illustrated in Fig. 21.

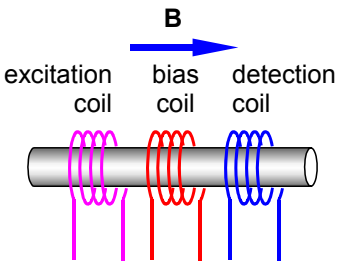

Figure 21. Principle configuration of a fluxgate magnetometer.

In its basic version, also called “peaking strip” [42], it consists of three coils wound around a ferromagnetic core: an excitation winding that produces an AC magnetic field well above the saturation field of the core, a detection winding that picks-up the excitation voltage and is used to detect the zero field condition and to generate an error signal proportional to the field, and a DC bias coil that improves the linearity of the device by creating and maintaining zero field in the core. The current in the bias winding is adjusted based on the error signal from the detection winding. At

equilibrium, once the error signal is zero, the field to be measured is equal (and opposite) to the field generated by the bias coil. The magnetometer reading provides hence a signal proportional to the field.

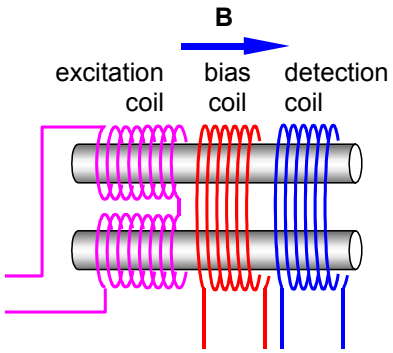

Figure 22. Fluxgate magnetometer built from two ferromagnetic needles.

In practice the coils are wound coaxially in subsequent layers to minimise stray field and maximise mutual inductances. Two ferromagnetic needles are used in order to avoid the distortion of the background field due to the presence of the probe, see Fig. 22. The excitation coil is wound around each needle, but the direction of the winding of the coils is reversed. The AC current in the excitation coil magnetizes the two needles with the same strength, but opposite direction. The detection and bias coils are wound surrounding the two ferromagnetic cores and the excitation coil. The detection coil thus senses the voltage induced by the change of magnetization in both needles. In absence of an external field the total voltage seen by the detection coil is zero because the magnetic field in the two needles have the same strength but opposite direction. If on the other hand the cores are aligned with an external magnetic field, one core will produce a magnetic field in the same direction and will reinforce it, while the other will subtract to it. This difference generates a measurable signal in the detection coil that appears as a second harmonic of the excitation current and whose strength is proportional to the external magnetic field (see Fig. 23). As discussed above, the bias coil is powered with a DC current proportional to the error signal from the detection coil.

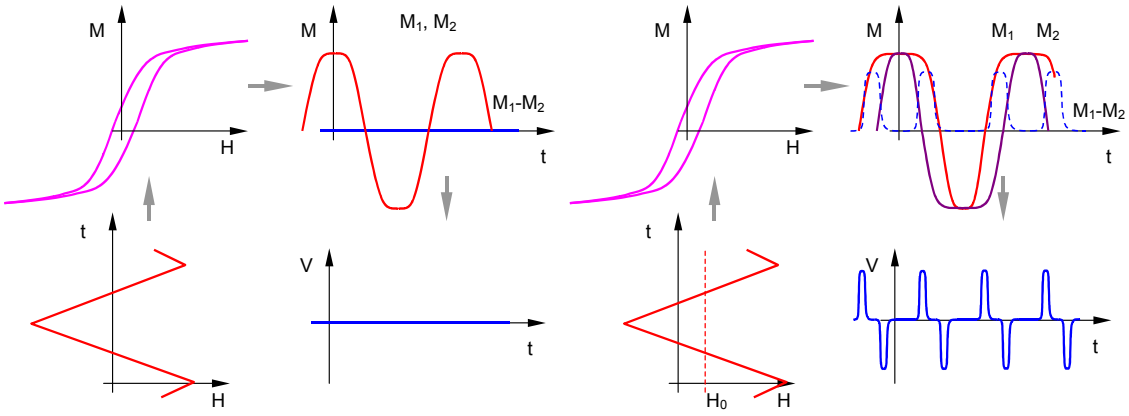

Figure 23. Working principle of the two-needles fluxgate magnetometer of Fig. 21 explained using a graphical construction. The magnetization of the two needles M_1 and M_2 is plotted in absence (left) and presence (right) of an external field $B_0 = \mu_0 H_0$. The voltage on the detection coil V is proportional to the time derivative of the difference of the two magnetizations M_1-M_2.

A fluxgate magnetometer of this type provides a measurement of the field component in the direction of the two needles and is a highly sensitive directional device. The bias coil is often combined with the

detection coil by powering it directly with a DC component proportional to its AC reading. Combining several magnetometers it is possible to sample the field in different directions, e.g. in three dimensions. The ferromagnetic needles can be substituted by a toroidal core partially covered by the detection coil. In this case the field component detected is the one normal to the direction of the winding of the detection coil. Using two detection coils wound at 90 degrees on the toroidal core it is possible to sense simultaneously two components of the field.

The first fluxgate magnetometers were built in the 1930's and largely developed during World War II. One of the applications was submarine detection from low-flying aircraft. The improvement of magnetic materials and detection electronics has lead to an improvement of sensitivity up to 0.1 nT. Because of the excellent sensitivity, small volume and weight and low cost, the fluxgate magnetometer is commonly used in the measurement of weak magnetic fields, such as earth field or rock layers. It can be used to detect small anomalies in magnetization such as generated by leakage earth current in power lines or the magnetic signature of vessels and weapons. Due to its directionality it is also used as a navigation instrument, to measure the geomagnetic field as well as for space applications, e.g. in the mapping of the interplanetary and planetary magnetic field.

Finally, it is worth to remember that the Direct Current Current Transformer (DCCT), commonly used for high-precision measurement of current, is based on the same principle of the fluxgate magnetometer. In the case of a DCCT the magnetic core has a toroidal shape, with the excitation and detection/bias coils wound around the toroid, as shown schematically in Fig. 24. The DCCT senses the weak magnetic field produced by a current conductor passing in the toroidal core. By careful arrangement of the conductor the magnetic field generated is perfectly linked with the magnetic core, while external fields have no influence. The signal on the bias coil is thus proportional to the current flowing in the conductor.

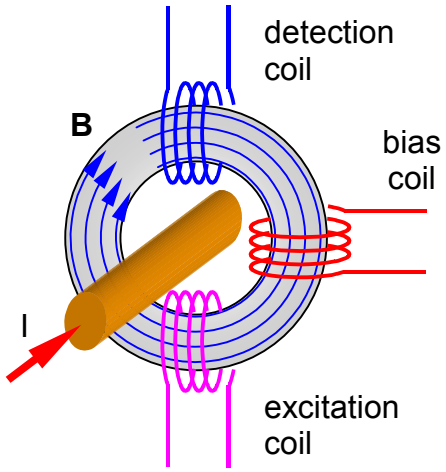

Figure 24. Principle of a DCCT, using the fluxgate magnetometer concept to measure the current passing in a conductor.

The range of fluxgate magnetometer is limited by the capability of the bias coil. The maximum field that can be measured is of the order of a few mT. The field range can be extended significantly by actively cooling the bias coil. The accuracy of the reading depends mainly on the calibration and on the stability of the device. Typical accuracy of commercial devices is in the 0.1 % to 1 % range (a few 1000's ppm). The volume sampled by the commercial probes ranges from a few to a few tens of mm^3. Finally, the bandwidth is typically from DC conditions to 1 kHz.

2.6 Magneto-inductance

Magneto-inductive magnetometers are relatively new devices [43,44], with the first patent issued in 1989. The magneto-inductive sensor detects a change in the inductance of a coil wound around a magnetic core whose permeability changes linearly over the range of measurement. This coil is an element of an L-R relaxation oscillator, as shown schematically in Fig. 25. The oscillation frequency is proportional to the external field to be measured. A DC bias can be applied to the coil to shift the working point of the magnetic core in a linear range of operation. The frequency can be monitored and measured to derive the corresponding field value by calibration. As for the fluxgate magnetometer, the sensor can be arranged to detect not only the magnitude but also the direction of the field. These magnetometers are gaining in popularity as they are easy in construction and relatively inexpensive. Magneto-inductive magnetometers have a limited operating range of typically 1 mT with a resolution in the μT range. Absolute accuracy is limited by calibration and stability issues.

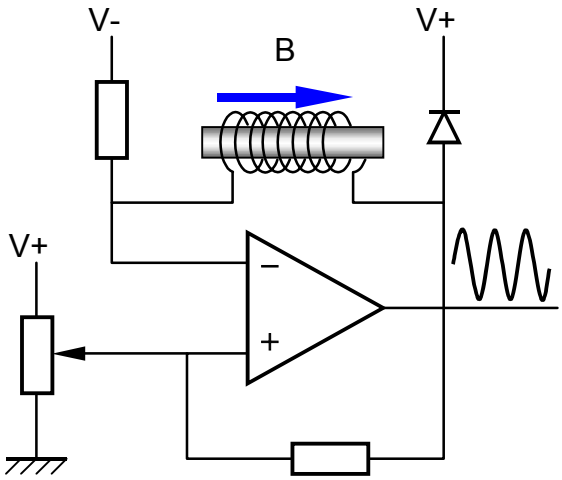

Figure 25. Principle of a magneto-inductive sensor. The sensor is the coil wound around a magnetic core. The oscillation frequency is proportional to the inductance of the sensor which in turn is affected by the applied field.

2.7 Superconducting Quantum Interference Device (SQUID)

2.7.1 Principle and applications

The Superconducting Quantum Interference Device (SQUID) is at present the device with the highest sensitivity to the magnetic field. The working principle of a SQUID rests on two physical phenomena typical of superconductors and accounted for only by quantum mechanics: flux quantization and Josephson tunneling. Flux quantization originates from the relation between magnetic flux and the phase of the wave function describing paired electrons in a superconductor. In the case of a superconducting ring encircling a normal-conducting region the change of phase δ along a closed path Γ that includes the hole can be expressed as a function of the magnetic flux φ linked with the same path as follows:

$$\delta = 2\pi \frac{\varphi}{\varphi_0} \tag{12}$$

where the quantity φ_0 is the so called flux quantum:

$$\varphi_0 = \frac{h}{2e} \tag{13}$$

whose value in SI units is 2.07×10^{-15} Wb. In order to avoid interference in the wave function, and thus to have a finite probability for the paired state, the phase difference must be an integer multiple of 2π. The consequence is that the magnetic flux inside the superconducting ring can only take integer multiples of φ_0. It is for this reason that magnetic field penetration in a bulk superconductor can only take place discretely, with the field entering in frozen flux lumps, the fluxoids, enclosing a magnetic flux equal to φ_0.

The second phenomenon, Josephson tunneling, is named after Brian Josephson who predicted in 1962 that pairs of superconducting electrons in two bulk superconducting material would tunnel through a thin, normal conducting barrier separating them [45]. The assembly of the superconducting materials and the normal conducting barrier is called a *Josephson junction*. Because of the pairing mechanism, a DC superconductive current can flow across the junction. The maximum current I that can flow without voltage development depends on the phase difference δ between the wave functions describing the paired electrons on the two sides of the resistive barrier. The dependence is periodic in δ:

$$I = I_c \sin(\delta) \tag{14}$$

where I_c is the maximum critical current of the junction. Above the critical current a resistive voltage is developed and the junction behaves as an ohmic conductor.

A SQUID consists schematically of a superconducting ring separated by one (RF SQUID) or two (DC SQUID) Josephson junctions. Although RF SQUIDs were the first to be used for magnetometry, present systems are largely based on DC SQUIDs. For this reason we will limit our discussion to DC SQUIDs only. Details and a more precise treatment on the principles of operation of SQUIDs can be found in [46] and [47].

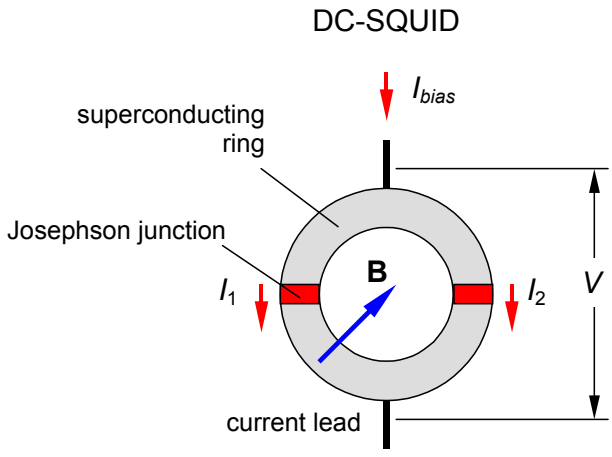

Figure 26. Schematic geometry of a DC-SQUID consisting in a superconducting ring with two Josephson junctions.

In the case of the DC SQUID shown in Fig. 26 the critical current of the ring is given by the parallel of the critical currents of the two Josephson junctions I_1 and I_2. These in turn depend through the relation expressed in Eq. (13) on the phase differences δ_1 and δ_2 of the wave functions of paired electrons across the junctions. In the presence of an external magnetic field the integral δ of the phase of the wave function of paired electrons around the ring depends on the flux linked by the ring in accordance with Eq. (12), where now however we need to consider the phase jumps across the two junctions:

$$\delta + \delta_1 - \delta_2 = 2\pi \frac{\varphi}{\varphi_0} \tag{15}$$

The flux quantization condition, requesting that the total phase change is an integer multiple of 2π, applies to the above equation and imposes a constraint between the single-phase jumps across the junctions. This constraint, combined with the periodic dependence of the maximum currents of each junction expressed by Eq. (14), results in a flux-dependent modulation of the critical currents of the two junctions. It can be shown in particular that the total critical current of the ring, under simple conditions of identical junctions and negligible loop inductance, is given by:

$$I = 2I_c \left| \cos\left(\pi \frac{\varphi}{\varphi_0} \right) \right| \tag{16}$$

which is a periodic function with period φ_0 and maximum value $2I_c$ shown in Fig. 27. To measure flux, the SQUID is powered as shown in Fig. 26 with a bias current I_{bias} close to the maximum critical current. The resistive voltage V appearing at the terminals of the SQUID is then also a periodic function of the magnetic flux, as shown schematically in Fig. 27.

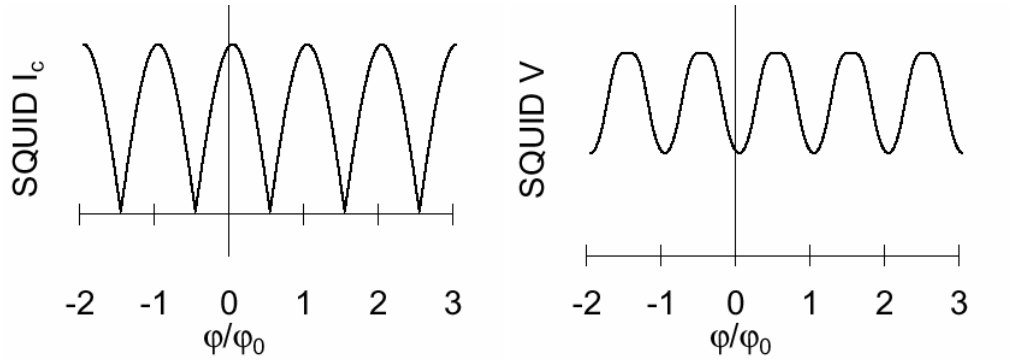

Figure 27. Critical current (left) and voltage (right) of a DC-SQUID as a function of the magnetic flux threading the ring.

Detecting the resistive voltage change it is hence possible to measure the flux linked by the SQUID. In practice the flux variation is measured using the voltage from the SQUID as an error signal for a feed-back coil magnetically coupled with the SQUID that adjusts until the feed-back flux cancels the external flux. The flux generated by the feed-back coil is then used as a measurement of the external flux. This zeroing technique makes possible to measure flux variations that are small fractions of the flux quantum.

Based on the measured flux change it is possible to derive the magnetic field as in the case of an induction coil. The main factors that govern the sensitivity of a SQUID are therefore the flux resolution and the SQUID area. The practical size of a SQUID is about 0.01 mm^2, and the field variation that can be detected by a bare device is in the pT range. The absolute accuracy of the device depends on the knowledge of the SQUID surface, but is usually not the main concern, as SQUIDS are mainly used for field measurements because of their extraordinary sensitivity. In order to further increase the sensitivity of the simple SQUID magnetometer described above, the flux seen by the superconducting ring can be amplified using a superconducting transformer. This consists of a detection coil wound with a superconducting wire connected to an input coil mutually coupled with the SQUID as shown in Fig. 28. Choosing properly the ratio of area and turns of the detection and input coils it is possible to amplify any field variation at the detection coil by a factor up to one

thousand. This gives a detection capability at the level of 10 fT for coil sizes of a few cm^2. Due to their exceptional sensitivity, SQUIDs are well suited for the measurement of the tiny magnetic fields associated with heart (100 pT) and brain (100 fT) activity. In addition they are used for fine magnetometry, non-invasive measurements and flaw detection. The bandwidth of a SQUID magnetometer is typically from DC to a few tens of kHz. Given the present rate of development in high-temperature superconductors and superconducting electronics, SQUIDs are expected to become more widespread in the future.

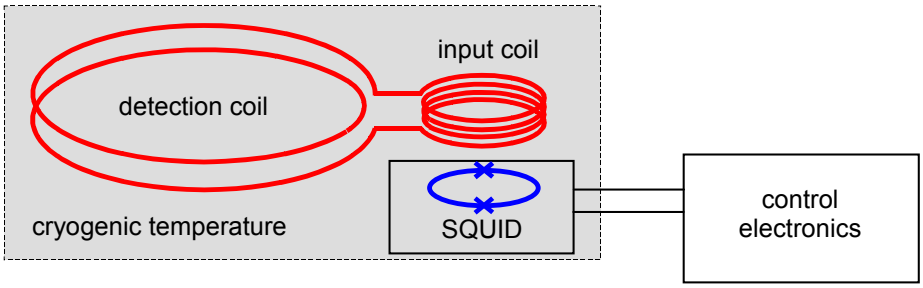

Figure 28. Coupling of a SQUID with a superconducting transformer consisting of a detection coil and an input coil that concentrates the magnetic flux at the SQUID.

2.8 Particle beams

The motion of elementary charged particles is another sensitive method to measure and map magnetic field over large volumes. As an example, low-energy electron beams are systematically used to map the field surfaces of thermonuclear fusion experimental devices with magnetic confinement. A diffused electron beam is injected in the plasma volume. The motion of the electrons takes place along the field lines, on the nested magnetic surfaces. Using transparent fluorescent meshes to detect the electrons it is possible to obtain a cross section of the field surfaces. The resulting maps are generally used to verify the regularity of the magnetic surfaces and the absence of magnetic island that could generate an instability in the thermonuclear plasma.

A second example is a method for the precise measurement of the beam position with respect to the magnetic center of quadrupole magnets installed in particle accelerators that has been developed over the last decade [48,49]. The procedure consists of modulating the field strength in individual lattice quadrupoles while observing the resulting beam orbit oscillations. Local DC orbit distortions are applied in the search for the magnetic center. This so-called K-modulation provides a perfect knowledge of the location of the particle beam with respect to the center of a quadrupole. In addition, it may provide other very useful observations for operation and adjustment of the accelerator [50]. This is obviously of particular importance for superconducting accelerators [51]. It is very difficult to provide a superconducting quadrupole magnet with a direct optical reference to its magnetic center, so errors caused by changes of temperature profiles and other phenomena may build up as time passes. The method may be further improved by synchronous detection of the oscillation, so that its phase can be identified. The sensitivity of the detection is impressive. Experience from LEP [52] showed that an absolute accuracy of 0.05 mm in both the vertical and horizontal plane could be obtained. Furthermore it was observed that a modulation of the quadrupole field of about 300 ppm could be clearly detected, which means that measurements may be carried out on colliding beams while particle physics experiments are taking place.

2.9 Magneto-optical measurement methods

Light propagation in matter is affected by the presence of a magnetic field, and this can be exploited to detect and measure the magnetic field itself. As light-based system have generally a high degree of electromagnetic compatibility and are fast, magneto-optical measurement find their application in

special and extreme operating conditions where measurement speed is important. The magneto-optical effect that is most widespread for field measurement is the Faraday rotation of the polarisation plane of light. The principle of an optical magnetometer based on Faraday rotation is shown in Fig. 29. A light beam is polarised on a plane before entering the detector proper. The detector itself consists of a transparent material (e.g. an optical fiber) placed in the magnetic field to be detected. The polarisation plane is rotated by the magnetic field component parallel to the direction of light propagation. The rotation θ of the polarisation plane is linearly proportional to the integrated field over the detector material, or:

$$\theta = v\int Bdl \tag{17}$$

vhere v is the material dependent Verdet constant. The light emerging from the detector is then analysed with an analyser and measured on a light intensity detector. As standard practice, the analyser is set at right angle with respect to the plane of polarisation, and the detector is used to find the minimum of the transmitted light intensity, thus increasing the resolution. This measurement principle has shown to be useful for measurements of transient magnetic fields [53,54], especially when high speed (sub-μs time scale) and ruggedness (e.g. explosive magnetic field generators) are important. It is however less convincing with respect to accurate measurement of field strength, as in general the rotation of the polarisation plane through practical thicknesses of optical materials is small, as shown by the values of the Verdet constant reported in Table 2. The uncertainties in the measurement of the angle of rotation of the polarisation plane, combined with the wavelength dependence of the Verdet constant, limit the typical accuracy of magneto-optical field measurements to fractions of percent at best (a few thousands of ppm).

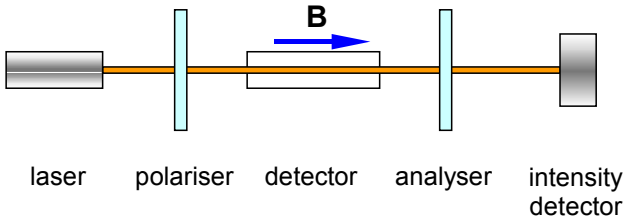

Figure 29. Working principle of magneto-optical field measurement based on the Faraday effect.

Table 2
Typical values of Verdet constant for optical materials, measured in visible light.

material	v (rad/T m)
water	3.8
glass	4…6
dense flint	25
quartz	4.8
NaCl	12
CaF_2	2.5
benzene	8.7

2.10 Field Imaging

The best known method for field imaging is made by spreading iron powder on a horizontal surface placed near a magnetic source, thus providing a simple picture of the distribution of flux lines. Another very classical way of observing flux-line patterns is to place a free-moving compass needle at

different points in the volume to be examined and note the direction of the needle. This compass method was applied, long before the discovery of electromagnetism, for studies of the variations in the direction of the earth's magnetic field. The magneto-optical rotation of the plane of polarization of polarized light (the Faraday effect described previously) is a classical method for the visualization of magnetic fields. A transparent container filled with a polarizing liquid and placed inside the magnet gap may visualize for example the field pattern in a quadrupole by observation through polarization filters placed at each end of the magnet. The rotation of the plane is proportional to the field strength and the length of the polarizing medium and may give a certain indication of the field geometry. A similar effect may be obtained by observing the light transmission through a colloidal suspension of magnetic particles, subject to the field [55,56]. An example of field imaging obtained using this method is shown in Fig. 30. The field pattern reported there has been obtained at RHIC using a ferro-fluid colloidal suspension contained in a cell placed in the warm bore of a quadrupole operated at a gradient of 75 T/m during cold test [57].

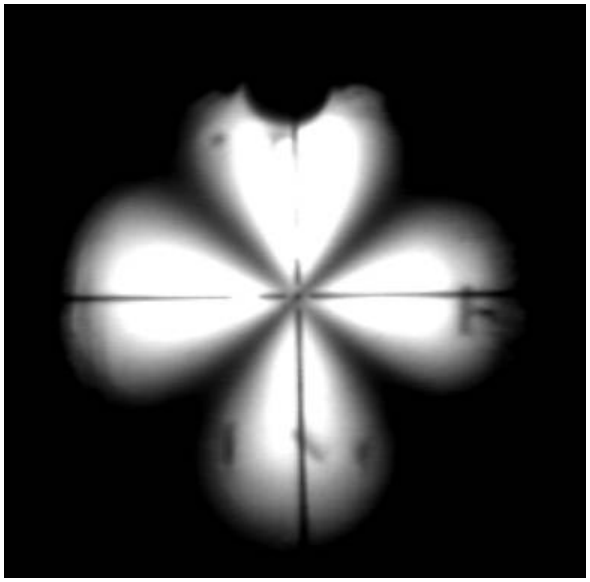

Figure 30. Polarised light pattern obtained using a ferro-fluid colloidal cell placed in the warm bore of a RHIC quadrupole powered at 75 T/m during tests at cryogenic temperature [57].

2.11 Other techniques

A plethora of different, alternative techniques can be used to measure magnetic field. Many of these techniques were either popular in the past, and have passed from practice, or are becoming increasingly attractive thanks to technological development, or again they are specially suited for particular applications. A few examples are listed below, once again not aiming at completeness:

Floating wire measurements were quite popular in the past [58]. If a current-carrying conductor is stretched in a magnetic field, it will curve subject to the electromagnetic force and describe the path of a charged particle with a momentum corresponding to the current and the mechanical tension in the wire. A flexible annealed aluminum wire was used in order to reduce effects of stiffness and gravity. This method has now been entirely replaced by precise field mapping and simulation of particle trajectories by computer programs.

Cantilever magnetometers sense the strength of a magnetic moment in a field gradient through the measurement of the magnetic force or the magnetic torque.

Magnetostriction has been used [59,60] to measure the magnetic field either detecting the magnetostrictive strain using a piezo-electric sensor or measuring the motion of a magnetostrictive ribbon using a tunneling tip.

Magneto-transistors and magneto-diodes are being developed. Semiconductors are sensitive to the magnetic field either through the Hall effect, or through the Suhl effect, a process by which the holes injected into an N-type semiconducting filament are deflected to the surface when a strong transverse magnetic field is applied to the semiconductor.

3. SUMMARY

Figure 31 reports an order-of-magnitude summary of the capability of the methods discussed in this note, in terms of measurement accuracy and measurement range.

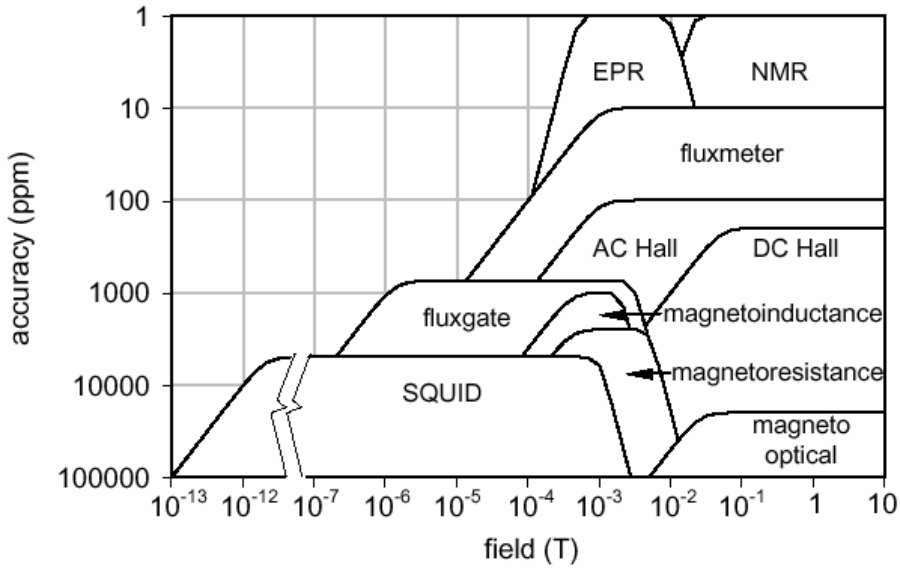

Figure 31. Overview of typical accuracy attainable with different magnetic measurement methods depending on the measured field. Note the jump by 5 orders of magnitude at the lower end of the magnetic field scale.

Proven measurement methods and powerful equipment is readily available for most of the measurement tasks related both to normal and superconducting magnets. It is therefore prudent to examine existing possibilities carefully before launching the development of a more exotic measurement method. Many unnecessary costs and unpleasant surprises can be avoided by choosing instrument, which are commercially available. The measurement methods described above are complementary and a well-chosen combination of two or more of these will certainly meet most requirements.

REFERENCES

[1] Nuclear Instruments and Methods in Physics Research – Section A, Elsevier Science.
[2] Proc. of the International Magnet Technology Conferences, MT-1 (1965) to MT-17 (2001).
[3] Proceedings of Particle Accelerator Conferences, PAC-1 (1965) to PAC-19 (2001).
[4] Proceedings of European Particle Accelerator Conferences, EPAC-1 (1988) to EPAC-18 (2002).
[5] Proc. of the International Magnetic Measurement Workshops, IMMW-1 (1977) to IMMW-12 (2001).

[6] Proceedings of CERN Accelerator School on Magnetic Measurement and Alignment, S. Turner ed., CERN-92-05, 1992.
[7] Proceedings of CERN Accelerator School on Measurement and Alignment of Accelerator and Detector Magnets, S. Turner ed., CERN-98-05, 1998.
[8] J.J. Rabi, J.R. Zacharias, S. Millman, P. Kusch, "A new method of measuring nuclear magnetic moment", Phys. Rev., **53**, 318, 1938.
[9] F.F. Bloch, W.W. Hansen, M. Packard, "Nuclear Induction", Phys. Rev., **69**, 127, 1946.
[10] F.F. Bloch, W.W. Hansen, M. Packard, "The Nuclear Induction Experiment", Phys. Rev., **70**, 474, 1946.
[11] E.M. Purcell, H.C Torrey, R.V. Pound, "Resonance Absorption by Nuclear Magnetic Moments in a Solid", Phys. Rev., **69**, 37-38, 1946.
[12] NIST Journal, **95** (5), 521, 1990.
[13] C. Reymond, "Magnetic Resonance Techniques", CERN Accelerator School on Measurement and Alignment of Accelerator and Detector Magnets, CERN-98-05, 219-231, 1998.
[14] W.G. Clark, T. Hijmans, W.H. Wong, "Multiple Coil Pulsed NMR Method for Measuring the Multipole Moments of Particle Accelerator Bending Magnets", J. Appl. Phys. **63**, 4185-4186, 1988.
[15] W.G. Clark, J.M. Moore, W.H. Wong, "Multiple Coil Pulsed Magnetic Resonance Method for Measuring Cold SSC Dipole Magnet Field Quality", Supercollider 2: Proc. of the 2nd International Industrial Symposium on the Supercollider, Miami Beach, USA 405-414, 1990.
[16] G. Suryan, "Nuclear Resonance in Flowing Liquids", Proc. Indian Acad. Sci., A33, 107-111, 1951.
[17] C. Sherman, "High-Precision Measurement of the Average Value of a Magnetic Field over an Extended Path in Space", Rev. Sci. Instr., **30**, 568-575, 1959.
[18] J.M. Pendlebury, K. Smith, P. Unsworth, G.L. Greene, W. Mampe, "Precision Field Averaging NMR Magnetometer for Low and High Fields, using Flowing Water", Rev. Sci. Instr., **50**, 535-540, 1979.
[19] L. Jansak, J. Kokavec, J. Kvitkovic, P. Galbraith, K.N. Henrichsen, "Low Field NMR Magnetometry using Flowing Water", Proceedings of the International Conference on Measurement, Measurement 97, Smolenice, Slovakia, 328-331, 1997.
[20] W. Weber, "Ueber die Anwendung der Magnetischen Induktion auf Messung der Inklination mit dem Magnetometer", Annalen der Physik, **2**, 209-247, 1853.
[21] M.I. Green, "Search Coils", CERN Accelerator School on Measurement and Alignment of Accelerator and Detector Magnets, CERN-98-05, 143-173, 1998.
[22] M.W. Garrett, "Axially Symmetric Systems for Generating and Measuring Magnetic Fields", Part I, Appl. Physics, **22** (9), 1091, 1951.
[23] W.F. Brown, J.H. Sweer, "The Fluxball", Rev. Sci. Instr., **16**, 276, 1945.
[24] B. de Raad, "Dynamic and Static Measurements of Strongly Inhomogeneous Magnetic Fields", Ph.D. Thesis, Delft University, 1958.
[25] G.H. Morgan, Proc. of 4th Int. Mag. Techn. Conf., USAEC CONF-720908, 787, 1972.
[26] Z.R. Wolf, et al., "Magnetic Measurement Instrumentation Development at the SSC", Supercollider **4**, 467-474, 1992.
[27] D. Zangrando, R.P. Walker, "A Stretched Wire System for Accurate Integrated Magnetic Field Measurements in Insertion Devices", Nucl. Instr. and Meth., A **376**, 275-282, 1996.
[28] W.C. Elmore, M.W. Garrett, "Measurement of Two-Dimensional Fields", Part I: Theory, Rev. Sci. Instr., **25**, 480-485, 1954.
[29] I.E. Dayton, F.C. Shoemaker, R.F. Mozley, "Measurement of Two-Dimensional Fields, Part II: Study of a Quadrupole Magnet", Rev. Sci. Instr., **25**, 485-489, 1954.
[30] A.K. Jain, "Harmonic Coils", CERN Accelerator School on Measurement and Alignment of Accelerator and Detector Magnets, CERN-98-05, 175-217, 1998.
[31] R.A. Beth, "Complex Representation and Computation of Two-Dimensional Magnetic Fields", J. Appl. Phys, **37**, 2568-2571, 1966.

[32] E.H. Hall, “On a New Action of the Magnet on Electric Currents”, Am. J. Math., **2**, 287, 1879.
[33] G.L. Pearson, “A Magnetic Field Strength Meter Employing the Hall Effect in Germanium”, Rev. Sci. Instr., **19**, 263, 1948.
[34] J. Hauesler, H.J. Lippmann, ”Hallgeneratoren mit Kleinem Lineariserungsfehler, Solid State Electron”, **11**, 173-182, 1968.
[35] C. Goldberg, R.E. Davis, “New Galvanometric Effect”, Phys. Rev., **94**, 1121-1125, 1954.
[36] B. Berkes, “Hall generators”, CERN Accelerator School on Magnetic Measurement and Alignment, CERN-92-05, 167, 1992.
[37] J. Kvitkovic, “Hall generators”, CERN Accelerator School on Measurement and Alignment of Accelerator and Detector Magnets, CERN-98-05, 233-249, 1998.
[38] J. Babiskin, “Oscillatory Galvanomagnetic Properties of Bismuth Single Crystals in Longitudinal Magnetic Fields”, Phys. Rev., **107**, 981-992, 1957.
[39] H.P.R. Frederikse, W.R. Hosler, “Oscillatory Galvanomagnetic Effects in n-Type Indium Arsenide,” Phys. Rev., **110**, 880-883, 1958.
[40] W. Thomson, “On the Magnetization of Electric Conductivity of Metals”, Philosoph. Trans., **146**, 736-751, 1856.
[41] M.N. Baibich, et al., “Gian Magnetoresistance of (001)Fe/(001)Cr Magnetic Superlattices”, Phys. Rev. Lett., **61**, 2472-2475, 1988.
[42] J.M. Kelly, “Magnetic Field Measurements with Peaking Strips”, Rev. Sci. Instr., **22**, 256-258, 1958.
[43] M.J. Caruso, T. Bratland, C.H. Smith, and R. Schneider, “A New Perspective in Magnetic Field Sensing, Sensors Online”, December 1998, http://www.sensorsmag.com/articles/1298/mag1298/index.htm.
[44] N.H. Kim, T. Hawks; “Digital compass and magnetometer having a sensor coil wound on a high permeability isotropic core”, US Patent No. 4,851,775, 1998.
[45] B.D. Josephson, Phys. Lett., 1, 251-253, 1962.
[46] J. Clarke, “SQUID Sensors: Fundamentals, Fabrication and Applications”, H. Weinstock ed., 1-62, Kluwer Dordrecht, 1996.
[47] P. Carelli, G. Paterno, “Macroscopic Quantum Interference: DC-SQUID, in Principles and Applications of Superconducting Quantum Interference Devices”, A. Barone ed., World Scientific, 1992.
[48] D. Rice, G. Aharonian, K. Adams, M. Billing, G. Decker, C. Dunnam, M. Giannella, G. Jackson, R. Littauer, B. McDaniel, D. Morse, S. Peck, L. Sakazaki, J. Seeman, R. Siemann, R. Talman, “Beam Diagnostic Instrumentation at CESR”, IEEE Trans. on Nucl. Sci., **30**, 2190-2192, 1983.
[49] P. Rojsel, “A Beam Position Measurement System Using Quadrupole Magnets Magnetic Centra as the Position Reference”, Nucl. Instr. and Meth., A **343**, 371-382, 1994.
[50] R. Brinkmann, M. Boge, “Beam-Based Alignment and Polarization Optimization in the HERA Electron Ring”, 4th European Particle Accelerator Conference, London, 938-940, 1994.
[51] J. Deregel, P. Genevey, J.-M. Rifflet, P. Galbraith, K.N. Henrichsen, “Proposal of a K-Modulation System for the LHC Quadrupoles”, CERN LHC Project Report 4, 1996.
[52] I. Barnett, A. Beuret, B. Dehning, P. Galbraith, K. Henrichsen, M. Jonker, M. Placidi, R. Schmidt, L. Vos, J. Wenninger, I. Reichel, F. Tecker, “Dynamic Beam Based Alignment”, presented at the 6th Beam Instrumentation Workshop, Vancouver, Canada, 1994.
[53] J. Malecki, M. Surma, J. Gibalewicz, “Measurements of the intensity of transient magnetic fields by the Faraday effect”, Acta Phys. Polon., 16 (1057) 151-156.
[54] J.L. Robertson, D.T. Burns, D. Hardie, “Measurements of a magnetic field integral using the Faraday effect”, Nucl. Instr. And Meth., 203 (1982) 87-92.
[55] J.K. Cobb, J.J. Muray, “Magnetic Center Location in Multipole Fields”, Nucl. Instr. and Meth., 46, 99-105, 1967.

[56] D. Trbojevic, P. Cameron, G.L. Ganetis, M.A. Goldman, R. Gupta, M. Harrison, M.F. Hemmer, F.X. Karl, A. Jain, W. Louie, S. Mulhall, S. Peggs, S. Tepikian, R. Thomas, P. Wanderer, "Alignment and Survey of the Elements in RHIC", 1995 Particle Accelerator Conference, Dallas, Texas, USA, 2099-2021, 1995.
[57] A. Jain, Private Communication, BNL, 2002.
[58] L.G. Ratner, R.J. Lari, "A precision system for measuring wire trajectories in magnetic fields", Proc. International Symposium on Magnet Technology, Stanford, USA (1965) 497-504.
[59] M.D. Mermelstein, A. Dandridge, "Low-Frequency Magnetic Field Detection with a Magnetostrictive Amorphous Metal Ribbon", Appl. Phys. Lett., 51 (7), 545-547, 1987.
[60] J.H. Wandass, J.S. Murday, R.J. Colton, "Magnetic Field Sensing with Magnetostrictive Materials Using a Tunneling Tip Detector, Sensors and Actuators", 19, 211-225, 1989.